

Intramolecular Carbinolamine and Imine Formation with Cobalt(III)-Amine Complexes. Synthesis, Structure, and Reactivity

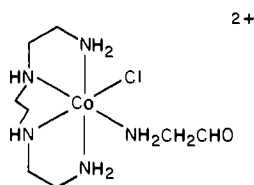
A. R. Gainsford, R. D. Pizer,¹ A. M. Sargeson,* and P. O. Whimp

Contribution from the Research School of Chemistry, The Australian National University, Canberra ACT 2600, Australia. Received July 9, 1980

Abstract: The $[\text{Co}(\text{NH}_3)_5(\text{NH}_2\text{CH}_2\text{COCH}_3)]^{3+}$ ion undergoes an intramolecular base-catalyzed cyclization reaction to produce a coordinated carbinolamine which undergoes a slower base-catalyzed dehydration to produce a chelated imine. The synthesis, characterization, and kinetics of formation of various reaction products are described. A study of the efficiency of carbinolamine production shows that the carbonyl group was captured on every other proton exchange. Several reactions of the imine product have been carried out including BH_4^- reduction and condensation with methyl vinyl ketone. A similar cyclization in the $[\text{Co}(\text{NH}_3)_5(\text{NH}_2\text{CH}_2\text{COC}_6\text{H}_5)]^{3+}$ ion to produce the analogous imine is also reported. A regio- and stereospecific intramolecular condensation of aminoacetaldehyde with the deprotonated secondary amine center trans to Cl^- in the α - $[\text{Co}(\text{trien})-(\text{NH}_2\text{CH}_2\text{CHO})\text{Cl}]^{2+}$ ion (trien = triethylenetetramine) also occurs. The reaction develops a chiral carbinolamine center with its oxygen atom oriented trans to the adjacent chelate. The α structure of the racemic carbinolamine product, ((*RRR*,*SSS*)-3-(2-amino-1-hydroxyethyl)-1,8-diamino-3,6-diazaoctane)chlorocobalt(III) bromide perchlorate, was established by a three-dimensional X-ray crystallographic analysis. The kinetics of the condensation were followed by pH-stat and buffer methods. The reaction rate-pH profile indicates a change in rate-determining step from base-catalyzed cyclization (at low $[\text{OH}^-]$) to dehydration of the *gem*-diol (at high $[\text{OH}^-]$). The carbonyl group was captured approximately once every 30 proton exchanges.

In the course of a program² designed to carry out organic reactions on metal ions, cobalt(III)-amine complexes containing N-bound aminoacetone, aminoacetophenone, and aminoacetaldehyde have been synthesized. In the free state all these organic molecules readily undergo intermolecular condensation reactions between the amine and carbonyl groups. These facile intermolecular reactions are inhibited by the irreversible coordination of their amine groups to the Co(III) moiety, since the metal ion consumes the lone pair of electrons on the free amine group and ligand exchange is negligible. Deprotonation of an adjacent coordinated amine center, however, allows the developed amido ion to attack the carbonyl group and make a chelate ring. This paper examines such intramolecular cyclization reactions, the intermediates, the products, and their rates of formation and decay on two types of cobalt(III)-amine complex.

The stereo- and regiospecificity of such reactions can be investigated in systems which permit more than one possible cyclization pathway. A suitable molecule for such a study is aminoacetaldehyde coordinated to a (triethylenetetramine)cobalt(III) moiety with the proposed structure



There is a prospect for condensation of the aldehyde at three amine centers cis to the aldehyde ligand. Addition at the NH *trans* to coordinated Cl^- yields the *t* isomer³ of the quinquidentate car-

binolamine $[\text{Co}(\text{trenenol})\text{Cl}]^{2+}$. Addition at the primary amine centers would give different *s* isomers³ of the same complex. There are interesting stereochemical possibilities in the reaction, and in this paper the properties and structures of the complexes are reported.

Experimental Section

Analytical grade reagents were used without further purification for all kinetic measurements. *d,l*-1-Amino-2-propanol (Research Organic/Inorganic Chemical Corp.), *d,l*-2-amino-1-phenylethanol (Aldrich Chemical Co. Inc.), and aminoacetaldehyde dimethyl acetal (Columbia Organic Chemicals Co. Ltd.) were used in the various syntheses. Spectrophotometric rate data and visible spectra were collected by using Cary 16K and 118C recording spectrophotometers. The ¹H NMR spectra were recorded at 100 MHz by using a JEOL Model JNM-MH-100 Minimar Spectrometer with sodium 3-(trimethylsilyl)propane-sulfonate as internal standard. The NMR signals were recorded in ppm (δ) positive downfield from the standard. The instrumentation for pH-stat titrations was used as described previously.⁴ Bio-Rad analytical Dowex 50W-X2 (200-400 mesh, Na^+ or H^+ form) and SP-Sephadex (C-25, Na^+ form) ion-exchange resins were used in the cation-exchange experiments. Infrared spectra were recorded on a Perkin-Elmer 457 spectrometer.

Syntheses. Racemic $[\text{Co}(\text{NH}_3)_5(\text{NH}_2\text{CH}_2\text{CH}(\text{OH})\text{CH}_3)](\text{ClO}_4)_3$ (I). To a solution of $[\text{Co}(\text{NH}_3)_5(\text{Me}_2\text{SO})](\text{ClO}_4)_3$ (25 g) in dimethyl sulfoxide (75 mL) was added *d,l*-1-amino-2-propanol (12 g), and the solution was stirred for 30 min. The mixture was added dropwise to a stirred solution of $\text{LiNO}_3 \cdot \text{H}_2\text{O}$ (10 g) in 95% ethanol (1 L). The gelatinous orange precipitate was collected and washed with absolute ethanol and then ether. (The filtrate is pink-red and apparently contains the O-bonded complex.) The crude complex was purified by dissolving it in

(3) Abbreviations used: *s* and *t* refer to the position of the Cl^- ion trans to a sec N or tert N in the product; *RR* defines the chirality of the N centers in one isomer and *SS* in the other; α and β refer to the various topological arrangements of the trien ligand about the Co(III) center (in the α structure the two terminal nitrogen donor atoms are trans to one another, the other two nitrogen donor atoms being in the equatorial plane; in the β structure, three nitrogen donor atoms are in the equatorial plane, the fourth (terminal) nitrogen is in an axial position (Buckingham, D. A.; Marzilli, P. A.; Sargeson, A. M. *Inorg. Chem.* 1967, 6, 1032); trien = $\text{NH}_2(\text{CH}_2)_2\text{NH}(\text{CH}_2)_2\text{NH}(\text{C}_6\text{H}_5)_2\text{NH}_2$; trenenol = $\text{NH}_2(\text{CH}_2)_2\text{N}(\text{CHOHCH}_2\text{NH}_2)\text{CH}_2\text{CH}_2\text{NH}(\text{CH}_2)_2\text{N}(\text{C}_6\text{H}_5)_2\text{NH}_2$; trenone = $\text{NH}_2(\text{CH}_2)_2\text{N}(\text{COCH}_2\text{NH}_2)\text{CH}_2\text{CH}_2\text{NH}(\text{CH}_2)_2\text{NH}_2$; tren = $\text{N}(\text{CH}_2\text{CH}_2\text{NH}_2)_3$; trenen = $\text{NH}_2(\text{CH}_2)_2\text{N}(\text{CH}_2\text{CH}_2\text{NH}_2)\text{CH}_2\text{CH}_2\text{NH}(\text{CH}_2)_2\text{NH}_2$; gly = glycinate anion; en = $\text{NH}_2(\text{CH}_2)_2\text{NH}_2$.

(4) Buckingham, D. A.; Davis, C. E.; Sargeson, A. M. *J. Am. Chem. Soc.* 1970, 92, 6159.

(1) On leave from the Department of Chemistry, City University of New York, Brooklyn College, Brooklyn, N.Y. 11210.

(2) (a) Harrowfield, J. MacB.; Sargeson, A. M. *J. Am. Chem. Soc.* 1979, 101, 1514. (b) *Ibid.* 1974, 96, 2634. (c) Golding, B. T.; Harrowfield, J. MacB.; Sargeson, A. M. *Ibid.* 1974, 96, 3003. (d) Bell, J. D.; Gainsford, A. R.; Golding, B. T.; Herlt, A. J.; Sargeson, A. M. *J. Chem. Soc., Chem. Commun.* 1974, 980. Buckingham, D. A.; Sargeson, A. M.; Zanella, A. J. *Am. Chem. Soc.* 1972, 94, 8246.

water (200 mL) and then slowly adding 70% HClO₄ (40 mL). The orange-yellow platelike crystals were collected, washed, and dried as above (9.8 g). A second fraction obtained on cooling the mother liquors to 0 °C was mainly the O-bound complex. Anal. Calcd for [Co(N₃H₁₅)(NC₃OH₉)](ClO₄)₃: Co, 11.39; H, 4.67; C, 6.96; N, 16.24; Cl, 20.55. Found: Co, 11.2; H, 4.7; C, 7.0; N, 16.1; Cl, 20.4 (ε₄₇₈ 68.7, ε₃₉₃ 8.4, ε₃₄₀ 60.3, and ε₃₀₂ 24.6 in 1 M HCl). ¹H NMR (1 M DCl): δ 1.17, 1.23 (sharp doublet, -CH(OH)CH₃, 3 protons), 2.6 (broad structured peak, CH₂ of amino alcohol ligand, 2 protons), 3.6 (br, NH₃ *cis* to amino alcohol, 12 protons), 3.9 (br, NH₃ *trans* to amino alcohol, 3 protons), 4.3 (br, NH₂ of amino alcohol, 2 protons). The resonances due to the methine proton were not perceived above the noise.

[Co(NH₃)₅NH₂CH₂COCH₃](ClO₄)₃. (II). Method 1. Compound I (5 g) was dissolved in 9 N H₂SO₄ (100 mL) at 25 °C, and a solution of Na₂Cr₂O₇·2H₂O (7.5 g) in 9 N H₂SO₄ (25 mL) was slowly added. The products were sorbed on a Dowex resin (5 × 5 cm), and elution was commenced by using 1 M HCl. The gray-green Cr(III) product (probably Cr(H₂O)₅SO₄⁺) that rapidly eluted from the resin was discarded. The Co(III) species were then eluted with 4 M HCl, and the eluate (250 mL) was cooled in an ice bath. HClO₄ (40 mL, 70%) was then slowly added, and the orange yellow product that deposited was collected and washed with absolute ethanol and then with ether. The crude product was dissolved in 0.1 N H₂SO₄ (40 mL), and a solution of NaClO₄·H₂O (7.5 g) and HClO₄ (7.5 mL, 70%) in water (10 mL) was slowly added. Yellow platelike crystals were deposited which were collected, washed and dried as above (4.3 g). This complex decomposes slowly at 25 °C to give some polymeric products, but it can be stored at 0 °C indefinitely. Anal. Calcd for [Co(N₅H₁₅)(NC₃OH₇)](ClO₄)₃: Co, 11.43; C, 6.99; H, 4.30; N, 16.30; Cl, 20.63. Found: Co, 11.2; C, 6.8; H, 4.4; N, 16.1; Cl, 20.6 (ε₄₇₈ 66.7, ε₃₉₃ 10.0, ε₃₄₀ 58.4, ε₃₀₉ 26.8 in 1 M HCl). ¹H NMR (1 M DCl): δ 2.18 (s, -CO-CH₃, 3 protons), 3.41, 3.48, 3.55 (t, NH₂-CH₂-C=, 2 protons) superimposed on 3.6 (br, 5NH₃, 15 protons), 4.4 (br, NH₂ of aminoacetone ligand).

Method 2. [Co(NH₃)₅(Me₂SO)](ClO₄)₃ (4 g) and 2-(amino-methyl)-2-methyl-1,3-dioxalan^{2d} (1.6 g) were dissolved in Me₂SO (75 mL), and, after 20 min at ambient temperature, the solution was diluted to 400 mL with water and the Co(III) complex sorbed on Dowex resin (4 × 2 cm) and elution was commenced with 1 M HCl (100 mL). An orange tripositive species was eluted from the resin with 4 M HCl, and the eluate was reduced to dryness in a Büchi evaporator. The orange residue was dissolved in 0.1 M HCl (50 mL) and the product deposited as the perchlorate salt by the addition of excess 70% HClO₄. The complex was collected and dried as in method 1 (2.5 g). This product has ¹H NMR and visible spectra identical with the product obtained in method 1.

[Co(NH₃)₅NH₂CH₂COCH₃](ClO₄)₃·H₂O (III). The eluate from method 1 was reduced to dryness in a Büchi evaporator. The orange residue was dissolved in 0.1 M HCl (50 mL), and 12 M HCl (20 mL) was added. Acetone was slowly added to the warm stirred solution until the cloud point was reached. On cooling of the solution to 0 °C, the orange chloride salt that deposited was collected and washed with acetone and then ether (1.6 g). Anal. Calcd for [Co(N₅H₁₅)(NC₃OH₇)]Cl₃·H₂O: Co, 17.25; C, 10.55; H, 7.08; N, 24.61; Cl, 31.14. Found: Co, 17.5; C, 10.4; H, 7.1; N, 24.4; Cl, 31.2. This complex has ¹H NMR and visible spectra with that of the perchlorate salt.

[Co(NH₃)₄(NH₂CH₂C(OH)(CH₃)NH₂)](NO₃)₂(ClO₄) (IV). Compound II (1.4 g) was dissolved in 0.01 M HCl, and the stirred solution was adjusted to pH 5.25 by the addition of a 0.03 M pyridine solution in water. After 10 min (6t_{1/2}), the reaction was quenched by the addition of HClO₄ (15 mL, 70%) and NaClO₄·H₂O (30 g). The small quantity of precipitated complex was filtered off and discarded. The filtrate was diluted to 600 mL with water, and the Co(III) complex was sorbed on a Dowex resin (3 × 3 cm) and eluted with 4 M HCl. The solution containing the orange tripositive Co(III) complex was reduced to dryness in a Büchi evaporator (<45 °C). The crude product was crystallized as the dinitrate perchlorate salt. The product was dissolved in 0.01 M HClO₄ (15 mL), and it was added dropwise to a solution of LiNO₃·H₂O (3 g) and HClO₄ (3 mL, 70%) in 95% ethanol (55 mL). The yellow-orange powder that deposited was collected and washed with absolute ethanol and ether (1.0 g). The complex was stored at 0 °C since at ambient temperature it slowly decomposed. Anal. Calcd for [Co(N₄H₁₂)(N₂O₃H₁₀)](NO₃)₂(ClO₄): Co, 13.37; C, 8.18; H, 5.03; N, 25.43; Cl, 8.05. Found: Co, 13.4; C, 8.3; H, 4.9; N, 25.5; Cl, 8.1 (ε₄₇₁ 70.9, ε₃₈₉ 7.7, ε₃₃₈ 63.4, and ε₂₉₉ 29.6 in 1 M HCl). ¹H NMR (1 M DCl): δ 1.74 (s, -(OH)CH₃, 3 protons), 2.8 (broad structured peak, -CH₂-, 2 protons), 3.6 (br, 4NH₃, 12 protons), 5.2 (br, 2NH₂, 4 protons). Attempts to resolve this complex with a variety of anions (e.g., (-)[As-(catecholato)₃]⁻) were unsuccessful.

[Co(NH₃)₄(HN=C(CH₃)CH₂NH₂)](ClO₄)₃ (V). Compound II (2 g) was dissolved in water (50 mL), and the pH was adjusted to 9.5 by the

dropwise addition of 0.1 M Na₂CO₃ solution. A rapid orange to yellow color change was observed. After 5 min, the solution was strongly acidified by the addition of HClO₄ (15 mL, 70%). The yellow product that deposited was collected and washed with absolute ethanol and then ether. The crude product was purified from water (25 mL) by slowly adding NaClO₄·H₂O (12 g) and HClO₄ (3 mL, 70%). The hexagonal platelike yellow product that deposited was collected and dried as above (1.5 g). Anal. Calcd for [Co(N₄H₁₂)(N₂C₃H₈)](ClO₄)₃: Co, 11.84; C, 7.24; H, 4.05; N, 16.89; Cl, 21.38. Found: Co, 12.0; C, 7.0; H, 4.1; N, 16.8; Cl, 21.4 (ε₄₆₅ 82.3, ε₃₈₅ 10.4, ε₃₃₂ 77.1, and ε₂₈₄ 11.1 in 1 M HCl). ¹H NMR (1 M DCl): δ 2.37 (s, CH₃-C=N, 3 protons), 3.36, 3.57 (br, overlapping NH₃ resonances; 12 protons), 3.97, 4.03, 4.09 (triplet, NH₂-CH₂-C=, 2 protons), 5.23 (br, NH₂-CH₂-, protons), 9.95 (br, HN=C, 1 proton). IR: ν_{C=N} 1672 cm⁻¹.

[Co(NH₃)₄(NH₂CH(CH₃)CH₂NH₂)](ClO₄)₃ (VI). Compound V (0.6 g) was dissolved in water (30 mL), and NaBH₄ (0.3 g) was added. The mixture was stirred for 1 min (H₂ evolved), and then the Co(III) complexes were rapidly sorbed on a Dowex resin (3 × 1 cm, Na⁺ form) and eluted with water (200 mL). The tripositive Co(III) complexes were eluted from the resin with 4 M HCl, and the eluate was reduced to dryness in a Büchi evaporator. ¹H NMR spectroscopy of the residue shows that the imine has only been 60% reduced, and some coordinated NH₃ was lost during the reduction. The mixture of complexes was sorbed onto a Sephadex resin (75 × 3 cm), and it was eluted with 0.2 M NaClO₄ (pH 5.5). Three bands separated: band 1 (pink) was eluted first and was probably a species resulting from ammonia loss; band 2 (yellow) was unreacted imine complex; band 3 (orange-yellow) was reduced imine complex. Bands 1 and 2 were discarded, and band 3 was sorbed on a Dowex resin (3 × 1 cm, H⁺ form) and the Co(III) complex eluted from the resin with 4 M HCl. The eluate was reduced to dryness in a Büchi evaporator. The residue was dissolved in the minimum volume of water, and HClO₄ (5 mL, 70%) was added. After the solution was cooled to 0 °C, the yellow product that deposited was collected and washed with ethanol and then ether (0.2 g). Anal. Calcd for [Co(N₄H₁₂)(N₂C₃H₁₀)](ClO₄)₃: Co, 11.80; C, 7.21; H, 4.44; N, 16.82; Cl, 21.29. Found: Co, 11.8; C, 7.0; H, 4.5; N, 16.7; Cl, 20.9 (ε₄₆₉ 73.1, ε₃₉₁ 19.0, ε₃₃₈ 70.5, and ε₂₉₄ 39.6 in 1 M HCl). ¹H NMR (1 M DClO₄): δ 1.42, 1.48 (sharp doublet, >CHCH₃, 3 protons), 2.55-3.45 (multiple peaks of >CH- and -CH₂-, 3 protons), 3.65 (br, 4NH₃ resonances, 12 protons), 5.0 and 5.2 (br, -NH₂ resonances, 2 protons each). These spectra are in good agreement with literature values.⁵

[Co(NH₃)₃(HN=C(CH₃)CH₂CH₂N=C(CH₃)CH₂NH₂)](ClO₄)₃ (VII). Compound V (1.0 g) was dissolved in 0.5 M Na₂CO₃/0.5 M NaHCO₃ (pH ~10), and methyl vinyl ketone (CH₃COCH=CH₂, 2.5 g) was added. The mixture was sealed and shaken continuously for 7 days. The mixture was diluted to 1 L and sorbed on a Dowex resin (4 × 1 cm, Na⁺ form). Elution was commenced with 1 M HCl (500 mL), the yellow effluent indicating the presence of polymeric organic species. Some Co(II) was also eluted at this stage. The Co(III) complexes were eluted from the column with 4 M HCl, and the eluate was reduced to dryness in a Büchi evaporator. The residue was dissolved in water (250 mL) and sorbed on a Sephadex resin (35 × 3.5 cm), and elution was commenced with 0.3 M NaBr. Three bands separated and the eluates containing each species were passed through a Dowex resin (2 × 1.5 cm) to sorb the Co(III) species. These complexes were eluted with 4 M HCl. After the eluates were reduced to dryness in a Büchi evaporator, ¹H NMR spectra gave the following results: band 1 (yellow, ~20% of product), 2 methyl resonances (~2.5) plus new methylene resonances; band 2 (yellow, ~70% of product), starting material; band 3 (orange, ~10% of product), only one NH₃ resonance, probably Co(NH₃)₆³⁺. The fractions from bands 2 and 3 were discarded; that from band 1 was dissolved in water (10 mL) and HClO₄ (8 mL, 70%) was slowly added. After the solution was cooled in an ice bath, the orange crystals that deposited were collected and washed with absolute ethanol and then ether (0.2 g). Anal. Calcd for [Co(N₃H₉)(N₂C₇H₁₅)](ClO₄)₃: Co, 10.72; C, 15.30; H, 4.40; N, 15.29; Cl, 19.35. Found: Co, 10.6; C, 15.2; H, 4.7; N, 15.6; Cl, 19.3 (ε₄₅₁ 94.0, ε₃₈₀ 14.0, ε₃₂₉ 89.9, and ε₂₉₃ 32.0 in 1 M HCl). ¹H NMR (1 M DClO₄): δ 2.46, 2.70 (sharp imine methyl resonances, 3 protons each), 3.0-3.3 (broad structured peaks, 10 protons, mutually *trans* ammonias plus -CH₂-CH₂-), 3.8 (br, NH₃ *trans* to -N=C-, 3 protons), 4.29, 4.35, 4.41 (t, NH₂-CH₂-C=N, 2 protons), 5.6 (br, -NH₂, 2 protons), 10.2 (br, HN=C, 1 proton).

[Co(NH₃)₄(NH=C(CH₃)C(CH₂OH)₂NH₂)](ClO₄)₂·0.5H₂O (VIII). Compound V (0.5 g) was dissolved in formaldehyde solution (36-38% in water, 60 mL), and 0.880 M NH₃ was added dropwise to pH 10.2 (~25 mL), during which time the color changed from yellow to an intense brown. After 30 min, the solution was diluted to 300 mL with

(5) Buckingham, D. A.; Durham, L.; Sargeson, A. M. *Aust. J. Chem.* 1967, 20, 257.

water, and the cobalt species were sorbed on a Dowex resin (4 × 2 cm). Elution with 1 M HCl (200 mL) gave some $\text{Co}(\text{H}_2\text{O})_6^{2+}$, and the orange-yellow tripositive $\text{Co}(\text{III})$ species were stripped from the resin with 4 M HCl. The eluate was reduced to dryness in a Büchi evaporator, and the residue was sorbed on a Sephadex resin (40 × 1.5 cm) and eluted with 0.075 M trisodium citrate. A series of pink bands (minor aquo/hydroxo products) were quickly eluted from the resin and discarded. These bands were followed by a slow moving broad yellow band which showed no clear separation of species present. This band was sorbed on a Dowex resin (4 × 2 cm) eluted with 1 M HCl (200 mL) to remove Na^+ and then with 4 M HCl. The eluate was reduced to dryness in a Büchi evaporator. The residue was dissolved in water (10 mL), and HClO_4 (10 mL, 70%) was added. The precipitated yellow salt was collected and washed with ethanol and then ether (0.1 g). ^1H NMR spectroscopy indicated that this salt was $[\text{Co}(\text{NH}_3)_6](\text{ClO}_4)_3$. The mother liquor was diluted with water to 100 mL, sorbed on a Dowex resin (2 × 1 cm), and eluted with 1 M HCl (50 mL) and then 4 M HCl. After the eluate was reduced to dryness, the residue was dissolved in water (5 mL) and NaI (1 g) and $\text{NaClO}_4 \cdot \text{H}_2\text{O}$ (2.5 g) added. When the solution was cooled to 0 °C, the yellow crystalline salt that deposited was collected and washed with absolute ethanol and then ether (0.25 g). Attempts to crystallize the iodide, perchlorate, dithionate, bromide, or chloride salts of this complex were unsuccessful. Anal. Calcd for $[\text{Co}(\text{N}_4\text{H}_{12})(\text{N}_2\text{C}_5\text{O}_2\text{H}_2)](\text{ClO}_4)_2 \cdot 0.5\text{H}_2\text{O}$: Co, 9.92; C, 10.11; H, 4.24; N, 14.15. Found: Co, 9.9; C, 10.1; H, 4.3; N 14.0 (ϵ_{460} 90.1, ϵ_{385} 22.7, ϵ_{328} 95.6, and ϵ_{299} 52.6 in water, pH 5). ^1H NMR (0.1 M DCl): δ 2.51 (s, imine methyl, 3 protons), 3.44 (br, 2 NH_3 , 6 protons), 3.73 (br, 2 NH_3 , 6 protons) superimposed on 3.75, 3.87, 3.99, 4.11 (sharp AB quartet, 2- CH_2 -OH with diastereotopic splitting, 4 protons), 5.87 (br, - NH_2 , 2 protons), 10.95 (br, $\text{HN}=\text{C}$, 1 proton). On addition of NaHCO_3 to the NMR sample, all amine and imine protons exchange while resonances due to the methyl and hydroxymethyl groups are not affected.

$[\text{Co}(\text{NH}_3)_5\text{NH}_2\text{CH}_2\text{CH}(\text{OH})\text{C}_6\text{H}_5](\text{ClO}_4)_3$ (IX). $[\text{Co}(\text{NH}_3)_5(\text{Me}_2\text{SO})](\text{ClO}_4)_3$ (10 g) was dissolved in dry Me_2SO (30 mL), and 2-amino-1-phenylethanol ($\text{NH}_2\text{CH}_2\text{CH}(\text{OH})\text{C}_6\text{H}_5$, 3 g) was added. There was no immediate color change (cf. with $\text{NH}_2\text{CH}_2\text{CH}(\text{OH})\text{CH}_3$ (II)); the mixture was gently heated to 65 °C on a steam bath and maintained at this temperature for 15 min, in which time the color changed to brown and some ammonia was evolved. The cooled mixture was poured into absolute ethanol (800 mL) containing $\text{LiNO}_3 \cdot 3\text{H}_2\text{O}$ (10 g) and the flocculant precipitate obtained was collected and washed with absolute ethanol and ether. The crude complex was purified by dissolving it in water (~400 mL) and adding slowly a solution of $\text{NaClO}_4 \cdot \text{H}_2\text{O}$ (15 g) in 5 M HClO_4 (50 mL). The yellow platelike crystals that deposited were collected and washed with 2-propanol and then ether (4.2 g). Anal. Calcd for $[\text{Co}(\text{N}_5\text{H}_{15})(\text{NC}_6\text{OH}_1)](\text{ClO}_4)_2 \cdot 5(\text{NO}_3) \cdot 0.5\text{H}_2\text{O}$: Co, 10.18; C, 16.59; H, 4.87; N, 15.73; Cl, 15.31. Found: Co, 10.2; C, 16.4; H, 5.0; N, 15.5; Cl, 15.3 (ϵ_{477} 67.5, ϵ_{390} 6.9, ϵ_{336} 62.0, and ϵ_{327} 59.2 in 1 M HCl). ^1H NMR (1 M DCl): δ 2.8 (br, NH_3 *trans* to aminoalcohol, 3 protons), superimposed on 2.77, 2.86 (d, - CH_2 -, 2 protons), 3.7 (br, *cis* NH_3 groups, 12 protons), 4.5 (br, - NH_2 of aminoalcohol, 2 protons), 5.00, 5.06, 5.12 (sh, t, - CH -, 1 proton), 7.51 (sh, singlet, phenyl resonances, 5 protons).

$[\text{Co}(\text{NH}_3)_5\text{NH}_2\text{CH}_2\text{COC}_6\text{H}_5](\text{ClO}_4)_3$ (X). Compound IX (1.25 g) was dissolved in H_2SO_4 (3 M, 150 mL) and $\text{Na}_2\text{Cr}_2\text{O}_7 \cdot 2\text{H}_2\text{O}$ (2.5 g) was slowly added to the stirred solution. After 40 min, the solution was diluted to 3 L with water, the $\text{Co}(\text{III})$ and $\text{Cr}(\text{III})$ species present were sorbed on Dowex resin (6 × 2.5 cm), and elution was commenced with 1 M HCl. After all of the gray-green $\text{Cr}(\text{III})$ complex(es) had been eluted from the resin, the $\text{Co}(\text{III})$ complexes were eluted with 4 M HCl and the eluate was reduced to dryness in a Büchi evaporator (<45 °C). The residue was dissolved in 0.01 M HClO_4 (100 mL) and the platelike crystalline product deposited by the addition of HClO_4 (20 mL, 70%). After the solution was cooled to 5 °C, the product was collected and washed with 2-propanol and then ether (1.1 g) (store at 0 °C). Anal. Calcd for $[\text{Co}(\text{N}_5\text{H}_{15})(\text{NC}_6\text{H}_5\text{O})](\text{ClO}_4)_3$: Co, 10.20; C, 16.64; H, 4.19; N, 14.55; Cl, 18.41. Found: Co, 10.3; C, 16.4; H, 4.0; N, 14.1; Cl, 18.5 (ϵ_{475} 57.6, ϵ_{390} 8.9, ϵ_{332} 54.0, and ϵ_{325} 52.8 in 1 M HCl). ^1H NMR (1 M DCl): δ 3.85 (br, 5 NH_3 , 15 protons), 3.9–4.2 (complex multiplet, - CH_2 -, 2 protons), 4.8 (br, - NH_2 , 2 protons), 7.5–8.2 (multiple peaks, - C_6H_5 , 5 protons).

$[\text{Co}(\text{NH}_3)_4(\text{HN}=\text{C}(\text{C}_6\text{H}_5)\text{CH}_2\text{NH}_2)](\text{ClO}_4)_3 \cdot \text{H}_2\text{O}$ (XI). Compound X (0.5 g) was dissolved in 0.1 M HClO_4 (25 mL), and a solution of pyridine in water (0.1 M) was added to adjust and maintain the pH at 5.5 for 5 min. After dilution to 100 mL with water the complexes were sorbed on Dowex resin (2 × 2 cm, H^+ 50W-X2 form), and elution was commenced with 1 M HCl (200 mL). There was no evidence of $\text{Co}(\text{II})$ species, and the yellow tripositive $\text{Co}(\text{III})$ complex was eluted from the resin with 4 M HCl and recovered by evaporation of the eluate in a Büchi evaporator. The residue was dissolved in water (15 mL), and HClO_4 (10

mL, 70%) was added dropwise. The platelike yellow crystalline product that deposited was collected and washed with 2-propanol and then ether (0.4 g). When the condensation was carried out at pH >8, there was significant decomposition of the $\text{Co}(\text{III})$ complex, yielding ammonia and benzaldehyde. Anal. Calcd for $[\text{Co}(\text{N}_4\text{H}_{12})(\text{N}_2\text{C}_6\text{H}_{10})](\text{ClO}_4)_3 \cdot \text{H}_2\text{O}$: Co, 10.20; C, 16.64; H, 4.19; N, 14.55; Cl, 18.41. Found: Co, 10.3; C, 16.2; H, 4.1; N, 14.5; Cl, 18.6 (ϵ_{469} 76.0, ϵ_{391} 24.1, and ϵ_{330} 109 (sh) in 1 M HCl). ^1H NMR ($\text{Me}_2\text{SO}-d_6$): δ 3.4 (br, NH_3 resonances, 12 protons), 4.48 (structured peak, - CH_2 -, 2 protons), 5.42 (br, - NH_2 , 2 protons), 7.5–8.1 (multiple resonances of phenyl group, 5 protons), 10.96 (br, $\text{HN}=\text{C}$, 1 proton). This complex decomposed in water at pH ~7 and was of low solubility.

$(RR,SS)\text{-}\alpha\text{-}[\text{Co}(\text{trien})(\text{NH}_2\text{CH}_2\text{CH}(\text{OCH}_3)_2)\text{Cl}]\text{Br}_2 \cdot 3$ (XII). A suspension of finely ground $(RR,SS)\text{-}\alpha\text{-}[\text{Co}(\text{trien})\text{Cl}_2]\text{Cl}^{16}$ (18.6 g) in methanol (800 mL) containing $\text{NH}_2\text{CH}_2\text{CH}(\text{OCH}_3)_2$ (6.3 g) was gently refluxed for a period of 1½ h, during which time the violet starting material dissolved to form an intense red-violet solution from which violet platelets of $(RR,SS)\text{-}\alpha\text{-}[\text{Co}(\text{trien})(\text{NH}_2\text{CH}_2\text{CH}(\text{OCH}_3)_2)\text{Cl}]\text{Cl}_2$ gradually deposited. After the reaction mixture was cooled to 5 °C, the precipitate was collected, washed with absolute ethanol, and dried with ether. The crude material was recrystallized from water (350 mL) by the slow addition of aqueous NaBr (30 g in 120 mL). The pale pink-violet platelike crystals were collected, washed, and dried as above (16.5 g). Anal. Calcd for $[\text{Co}(\text{C}_6\text{H}_{18}\text{N}_4)(\text{NH}_2\text{CH}_2\text{CH}(\text{OCH}_3)_2)\text{Cl}]\text{Br}_2$: Co, 11.65; H, 5.78; C, 23.74; N, 13.91. Found: Co, 11.7; H, 5.6; C, 23.7; N, 14.1 (ϵ_{535} 105, ϵ_{424} 18.7, ϵ_{367} 102, and ϵ_{332} 42.5 in water pH 5.5). For ^1H NMR spectra, the poorly soluble bromide was converted to the more soluble perchlorate salt by dissolution in water at 35 °C and the addition of excess $\text{NaClO}_4 \cdot \text{H}_2\text{O}$ with cooling. Two treatments were necessary to remove all of the bromide. The sample was washed with absolute ethanol and then ether and dried in a vacuum desiccator. Anal. Calcd for $[\text{Co}(\text{C}_6\text{H}_{18}\text{N}_4)(\text{NH}_2\text{CH}_2\text{CH}(\text{OCH}_3)_2)\text{Cl}](\text{ClO}_4)_2$: Co, 10.81; H, 5.36; C, 22.04; N, 12.91. Found: Co, 10.7; H, 5.4; C, 22.0; N, 13.0. ^1H NMR (D_2O) (Figure 1): δ 2.4–3.1 (CH_2 of trien and aminoacetal), 3.24 (CH_3 singlet, 6 protons). The CH signal of the aminoacetal was buried under the CH_2 and CH_3 resonances. All >NH and - NH_2 protons were exchanged; the spectrum was also measured immediately after dissolution of the complex in 0.5 M DCl: δ 2.5 to 3.2 (CH_2 of trien and aminoacetal), 3.51 (CH_3 singlet, 6 protons), 4.27 (NH_2 of aminoacetal), 5.57 (2 NH_2 of trien), 6.17 (>NH *trans* to Cl^-), 6.65 (>NH *cis* to Cl^-). There was no evidence of isomeric impurities when the complex was eluted on Dowex or Sephadex resins (1 × 15 cm) with NaBr or NaClO_4 (1 M and 0.15 M (pH 6.5), respectively).

$(RR,SS)\text{-}\alpha\text{-}[\text{Co}(\text{trien})(\text{NH}_2\text{CH}_2\text{CHO})\text{Cl}]\text{Br}_2 \cdot 2\text{H}_2\text{O}$ (XIII). Compound XII (10 g) was dissolved in 1 M HCl (300 mL), and the solution was maintained at 25 °C for 24 h.⁷ After evaporation in a Büchi evaporator (<40 °C) the purple oil that remained was dissolved in 2 M HBr (30 mL) and NaBr (6 g) was added. After the solution was stirred and cooled to 5 °C, violet crystals were obtained which were washed with absolute ethanol and then ether (7.8 g). The complex was stored at 0 °C until required. At 20 °C the solid complex decomposes slowly to give some polymeric materials. Anal. Calcd for $[\text{Co}(\text{C}_6\text{H}_{18}\text{N}_4)(\text{NH}_2\text{CH}_2\text{CHO})\text{Cl}]\text{Br}_2 \cdot 2\text{H}_2\text{O}$: Co, 11.89; H, 5.49; C, 19.39; N, 14.13. Found: Co, 12.0; H, 5.6; C, 19.4; N, 13.8 (ϵ_{534} 106, ϵ_{424} 21.6, ϵ_{367} 106, and ϵ_{332} 53.7 in 1 M HCl). IR: $\nu_{\text{C}=\text{O}}$ 1715 cm^{-1} . ^1H NMR (1 M DClO_4): δ 2.6–3.9 (complex CH_2 of trien and aminoacetaldehyde), 4.16 (br, partially structured peak of aldehyde/*gem*-diol NH_2), 5.34, 5.38, 5.42 (triplet of - $\text{CH}_2\text{CH}(\text{OH})_2$), 5.30 (3 NH_2), 6.08 (>NH *trans* to Cl^-), 6.48 (>NH *cis* to Cl^-), 9.67 ($\text{HC}=\text{O}$) (Figure 1C). The relative intensities of the peak of the aldehyde and *gem*-diol protons indicate that in solution the complex exists principally in the hydrated (*gem*-diol) form.

$(RRR,SSS)\text{-}t\text{-}[\text{Co}(\text{trenenol})\text{Cl}](\text{Br})(\text{ClO}_4)_3$ (XIV). Compound XIII (8 g) was dissolved in water (500 mL) at 25 °C and the pH of the stirred solution was adjusted and maintained at 6.2 by the dropwise addition of 0.01 M NaOH. The complex was then sorbed on a cation resin (3 × 12.5 cm), and the violet $\text{Co}(\text{III})$ species was eluted with 1 M HCl (2 L). There was no evidence for the presence of mono- or tripositive ions. The eluate containing all dipositive ions was reduced to ca. 30 mL in a Büchi evaporator, and 95% ethanol (500 mL) and ether (500 mL) were added. The precipitated violet powder was collected and washed with absolute ethanol and then ether. The crude product was recrystallized by dissolving it in 1 M HClO_4 (120 mL) containing $\text{NaClO}_4 \cdot \text{H}_2\text{O}$ (25 g) and then adding dropwise a solution of NaBr (40 g) in water (100 mL) with stirring. When the solution was cooled, the violet-red crystalline product slowly deposited. It was collected, washed, and dried as above. A further

(6) Searle, G. H.; Sargeson, A. M. *Inorg. Chem.* 1967, 6, 787.

(7) The half-life for the acid catalyzed loss of the methyl acetal is approximately 3 h at 25 °C, observed by monitoring the ^1H NMR spectrum of the complex in 1 M DClO_4 .

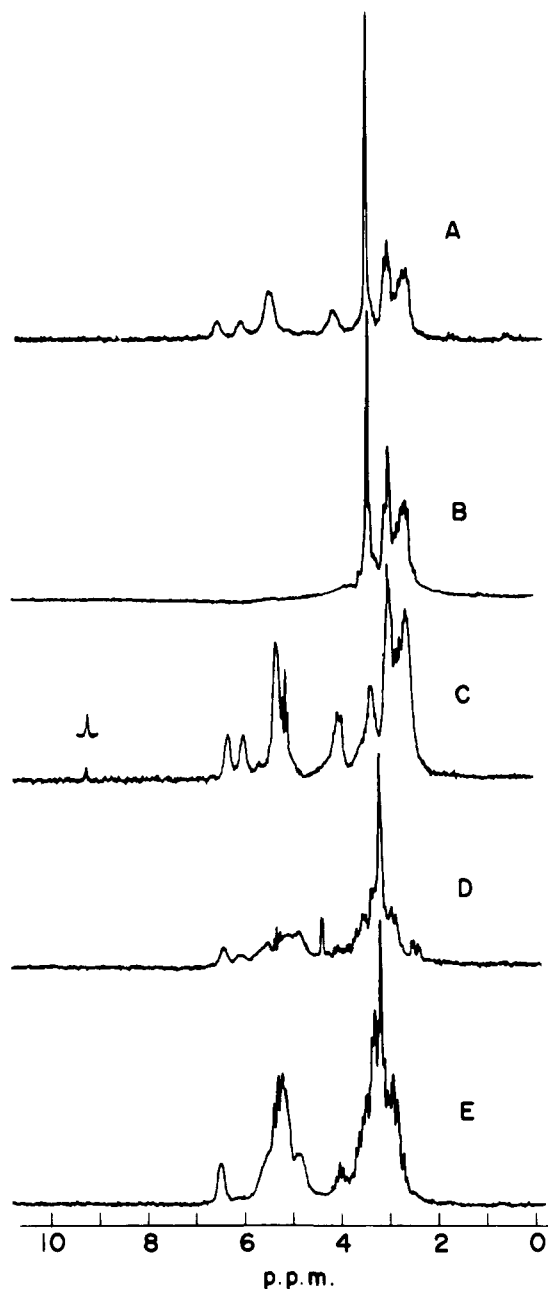


Figure 1. ^1H NMR spectra (100 MHz) for (A) $(RR,SS)\text{-}\alpha\text{-}[\text{Co}(\text{trien})(\text{NH}_2\text{CH}_2\text{CH}(\text{OCH}_3)_2\text{Cl})(\text{ClO}_4)_2]$ in 0.5 M DCl, (B) $(RR,SS)\text{-}\alpha\text{-}[\text{Co}(\text{trien})(\text{NH}_2\text{CH}_2\text{CH}(\text{OCH}_3)_2\text{Cl})(\text{ClO}_4)_2]$ in D_2O , (C) $(RR,SS)\text{-}\alpha\text{-}[\text{Co}(\text{trien})(\text{NH}_2\text{CH}_2\text{CHO})\text{Cl}]\text{Br}_2\cdot 2\text{H}_2\text{O}$ in 1 M DClO_4 , (D) $(RRR,SSS)\text{-}t\text{-}[\text{Co}(\text{trenenol})\text{Cl}]\text{Br}(\text{ClO}_4)$ in 1 M DCl, and (E) $(RRR,SSS)\text{-}t\text{-}[\text{Co}(\text{trenenone})\text{Cl}]\text{Br}_2$ in 1 M DClO_4 .

crop was obtained by the addition of NaBr (15 g) to the mother liquors (6.5 g). Anal. Calcd for $[\text{Co}(\text{C}_8\text{H}_{23}\text{N}_3\text{O})\text{Cl}](\text{Br})(\text{ClO}_4)$: Co, 12.30; H, 4.84; C, 20.06; N, 14.62. Found: Co, 12.2; H, 4.7; C, 20.1; N, 14.6 (ϵ_{331} 147, ϵ_{419} 20.1, ϵ_{361} 137, and ϵ_{329} 69.5 in 0.1 M HCl). ^1H NMR (1 M DCl): δ 2.3–4.2 (complex $-\text{CH}_2-$ resonances), 4.36, 4.39 (sh d, CH_2 adjacent to $\text{CH}(\text{OH})$), 4.9, 5.6, 6.0 (3NH_2), 6.6 ($>\text{NH}$), 5.28, 5.36, 5.44 (w t of $\text{CH}(\text{OH})$).

$(RR,SS)\text{-}t\text{-}[\text{Co}(\text{trenenone})\text{Cl}]\text{Br}_2$.² Compound XIV (2 g) was dissolved in 9 N H_2SO_4 (200 mL), and $\text{Na}_2\text{Cr}_2\text{O}_7$ (5 g) was added. The mixture was stirred at 25 °C for 2 h, and, after dilution to 2 L, it was sorbed on a Dowex resin (8 × 2.5 cm), washed well with water, and eluted with 1 M HCl. The green-violet Cr(III) product, probably $[\text{Cr}(\text{H}_2\text{O})_5(\text{SO}_4)]^+$, was eluted from the column and was discarded. The violet dipositive Co(III) species was then eluted with 2 M HCl (no evidence of tripositive species), and the eluate (200 mL) was reduced to dryness in a Büchi evaporator. The crude violet solid was recrystallized from the minimum volume of water (~30 mL) at 25 °C by the addition of excess NaBr (5 g). The product was collected and washed with ethanol and then ether (1.2 g). Anal. Calcd for $[\text{Co}(\text{C}_8\text{H}_{21}\text{N}_3\text{O})\text{Cl}]\text{Br}_2$:

Table I. Crystal Data

$a = 8.009$ (3) Å ^{a,b}	$c = 18.491$ (7) Å
$b = 11.228$ (4) Å	$\beta = 94.28$ (2) ^o
cryst color: violet-red	formula: $\text{C}_8\text{H}_{23}\text{BrCl}_2\text{CoN}_3\text{O}_5$
fw: 479.0	cell vol: 1658.2 Å ³
$\rho_{\text{obsd}} = 1.91$ (1) g cm ⁻³	$\rho_{\text{calcd}} = 1.92$ g cm ⁻³
space group: $P2_1/c$	$Z = 4$
(C_{2h}^2 , No. 14)	$\mu = 147.37$ cm ⁻¹

^a Cell dimensions were measured at 20 ± 1 °C by using Cu $K\alpha_1$ radiation ($\lambda = 1.5405$ Å). ^b Estimated standard deviations (in parentheses) in this and the following tables, and also in the text, refer to the least significant digit(s) in each case.

Co, 12.88; H, 4.63; C, 21.00; N, 15.31. Found: Co, 12.7; H, 4.6; C, 21.1; N, 15.2 (ϵ_{332} 137, ϵ_{423} 19.1, ϵ_{362} 129, and ϵ_{331} 72.1 in 0.1 M HCl). ^1H NMR (1 M DClO_4): δ 2.6–4.2 (complex $-\text{CH}_2-$ resonances), 5.20, 5.29, 5.38 (sh t, CH_2 adjacent to $>\text{C}=\text{O}$), 4.7–5.7 (4NH_2), 6.5 ($>\text{NH}$). IR: $\nu_{\text{C}=\text{O}}$ 1706 (ω) cm⁻¹.

Spectrophotometric Kinetic Measurements. (a) pH-stat. All reactions were followed at 25.00 ± 0.05 °C while maintaining the desired pH with a Radiometer pH-stat by using 0.1 M NaOH, $\mu = 1.0$ (NaClO_4). Little or no base was consumed (<10⁻³ mmol) in the course of the various reactions.

$[\text{Co}(\text{NH}_3)_5\text{NH}_2\text{CH}_2\text{COCH}_3]\text{Cl}_3\cdot\text{H}_2\text{O}$ (0.3 mmol) dissolved in 0.001 M HClO_4 (1 mL) was added to NaClO_4 (1 M, 50 mL), and the spectrophotometric data were recorded after the desired pH was established. The reaction was followed at 290 nm (condensation step) and 335 nm (dehydration step).

$(RR,SS)\text{-}\alpha\text{-}[\text{Co}(\text{trien})(\text{NH}_2\text{CH}_2\text{CHO})\text{Cl}]\text{Br}_2\cdot 2\text{H}_2\text{O}$ (0.2 mmol) was rapidly dissolved in NaClO_4 (1 M, 50 mL) which had been adjusted to the desired pH in a N_2 atmosphere. Spectrophotometric rate data were recorded after the desired pH had been reestablished. The reaction was followed at 530 nm.

(b) Stopped-Flow. Solutions were rapidly mixed at 25.00 ± 0.05 °C by using a stopped-flow reactor⁸ fitted with a 1-cm cell. pH was maintained by the use of buffer base ($\mu = 1.0$ (NaClO_4)). The value of the pH of the buffers was checked against the effluent solutions from the stopped-flow reactor and found to be unchanged (±0.02).

Solutions of $[\text{Co}(\text{NH}_3)_5\text{NH}_2\text{CH}_2\text{COCH}_3](\text{ClO}_4)_3$ and $[\text{Co}(\text{NH}_3)_4(\text{N}=\text{H}_2\text{CH}_2\text{C}(\text{OH})(\text{CH}_3)\text{NH}_2)](\text{NO}_3)_2\text{ClO}_4$ (8×10^{-3} M) in $\text{HClO}_4\text{NaClO}_4$ ($\mu = 1.0$) were rapidly mixed with the appropriate buffer base. Reactions were followed at 290 and 335 nm as above.

Proton-Exchange Rates. $[\text{Co}(\text{NH}_3)_5(\text{NH}_2\text{CH}_2\text{COCH}_3)]\text{Cl}_3\cdot\text{H}_2\text{O}$ was dissolved in pyrazole/DCl (pD 3.50 and 3.81, $\mu = 1.0$ at 25 ± 0.2 °C) and ^1H NMR spectra were measured every 60 min. The rates of *cis* NH_3 proton exchange and carbinolamine formation were determined by using log (area of amine resonance) and log (peak height) vs. time, respectively. The rates of exchange of methylene and methyl protons in $[\text{Co}(\text{NH}_3)_4(\text{N}=\text{H}(\text{C}(\text{CH}_3)\text{CH}_2\text{NH}_2)](\text{ClO}_4)_3$ were determined in $\text{Na}_2\text{CO}_3/\text{NaD-CO}_3/\text{D}_2\text{O}$ (pD 10.56, $\mu = 1.0$ at 25 ± 1 °C) by measuring the spectrum every 2 min for methylene exchange and then every 2 h for methyl exchange. Plots of log (peak height) vs. time were linear for at least 2 half-lives (assumed, pD = pH + 0.4).

$(RR,SS)\text{-}\alpha\text{-}[\text{Co}(\text{trien})(\text{NH}_2\text{CH}_2\text{CHO})\text{Cl}]\text{Br}_2\cdot 2\text{H}_2\text{O}$ (~50 mg) was dissolved in $\text{D}_2\text{O}/\text{DCl}$ (pD 4.9 at 32 ± 1 °C), and ^1H NMR spectra were measured. After 20 h at 25 °C, the sample showed signs of decomposition and the generation of the Co(II) species.

Collection and Reduction of X-ray Intensity Data. Approximate unit-cell dimensions for crystals of $[\text{Co}(\text{trenenol})\text{Cl}]\text{Br}(\text{ClO}_4)$ were obtained from preliminary Weissenberg ($hk0$ and $hk1$ data) and precession ($0kl$, $1kl$, $h0l$, and $h1l$ data) photographs which also showed systematic absences corresponding to space group $P2_1/c$ (C_{2h}^2 , No. 14).

The crystal chosen for data collection was transferred to a Picker FACS-I fully automatic four-circle diffractometer and was aligned with the crystal *a* axis and the instrumental Φ axis approximately coincidental. The unit-cell dimensions, together with estimated standard errors, and the crystal orientation matrix were obtained from the least-squares refinement⁹ of the 2θ , ω , χ , and Φ values found for 12 carefully centered high-angle reflections ($2\theta > 80^\circ$). Full details of the crystal data are collected in Table I.

Data collection details and experimental conditions are outlined in Table II.

Reflection intensities were reduced to values of $|F_o|$ and each reflection was assigned an individual estimated standard deviation.¹⁰ For this data

(8) Inoue, Y.; Perrin, D. D. *J. Phys. Chem.* **1962**, *66*, 1689.

(9) The programs contained in the Picker Corp. FACS-I Disk operating System (1972) were used for all phases of diffractometer control and data collection.

Table II. Data Collection Details

radiation	Cu K α
wavelength	1.5418 Å
monochromator	graphite crystal
tube takeoff angle	3.0°
cryst to counter dist	28.5 cm
scan technique	θ -2 θ scans
scan speed	2°/min
scan width	from 1.0° below the Cu K α_1 maximum to 1.0° above the Cu K α_2 maximum of each peak
scan range	3° \leq 2 θ \leq 125°
total bkgd counting time ^a	20 s
"standard" reflctn indices ^b	(0,2,12), (073), (502)
cryst stability	anisotropic decay of 3.5%, 4.5%, and 3.3% for the "standard" reflctns (0,2,12), (073), and (502), respectively
form of data collected	<i>hkl, hkl</i>
total no. of data collected	3119
no. with $I/\sigma(I) > 3.0$	1969
ρ^2	0.002

^a Backgrounds were counted on either "side" of each reflection (10 s each side) at the scan width limits and were assumed to be linear between these two points. ^b The three "standard" reflections were monitored after each 100 measurements throughout the course of data collection.

Table III. Starting Phases Generated by MULTAN

<i>h</i>	<i>k</i>	<i>l</i>	$ E $	ϕ , deg
2	12	-6	3.26	180
2	5	-9	2.66	0
0	11	2	2.53	0
1	1	5	2.21	180
1	2	2	1.96	0

set, the instrumental "uncertainty" factor (ϕ)¹¹ was assigned a value of (0.002)^{1/2}. During data collection, there was some crystal decomposition which was assumed to be anisotropic and 2 θ independent. Before further calculation, the intensity data were corrected for decomposition effects by using program SETUP 3. The reflection data were sorted to a convenient order, equivalent reflection forms were averaged, reflections for which $I/\sigma(I) < 3.0$ were discarded as being unobserved,¹⁰ and those reflections for which the individual background measurements differed significantly¹⁰ (i.e., $>4.0\sigma$) were also rejected. The statistical R factor¹⁰ (R_s) for the 1969 reflections of the terminal data set is 0.023.

Solution and Refinement of the Structure. After generation of normalized structure factors (using program EPROG), the structure was solved by using the MULTAN package of programs. MULTAN generated the phases shown in Table III, and these values were used to assign phases to 276 reflections with $|E| > 1.40$ which were then used as coefficients for a Fourier synthesis. The resulting "E map" showed the positions of the cobalt atom, the bromine atom, and the two chlorine atoms. The remaining atoms of the molecule were located from successive difference Fourier syntheses. With use of data which had been corrected for absorption effects, the structure was refined by block-diagonal least-squares methods to final unweighted and weighted R factors of 0.054 (R) and 0.064 (R_w), respectively. Atomic scattering factors for the nonhydrogen atoms were taken from the compilation of Cromer and Mann,¹² and those for all nonhydrogen atoms were corrected for the real and imaginary parts of anomalous scattering.^{13,14} Hydrogen atom

Table IV. Course of Refinement

set no.	conditns	no. of cycles	R^a	R_w
1	all atoms isotropic, no hydrogen atom contributions, individual weights ^b	6	0.123	0.139
2	all atoms anisotropic, ^c no hydrogen atom contributions, individual weights	5	0.086	0.112
3	at this point, reflection data were corrected for absorption effects: ^d all atoms isotropic, no hydrogen atom contributions, individual weights	6	0.070	0.095
4	all nonhydrogen atoms anisotropic, fixed isotropic, hydrogen atom contributions included, individual weights	12	0.054	0.064

^a $R = \Sigma ||F_o| - |F_c|| / \Sigma |F_o|$ and $R_w = \{\Sigma w[|F_o| - |F_c|]^2 / \Sigma w|F_o|^2\}^{1/2}$, where $|F_o|$ and $|F_c|$ are the observed and calculated structure factors, respectively. The function minimized during least-squares refinement was $\Sigma w(|F_o| - |F_c|)^2$. ^b Individual weights of the form $w = [\sigma(F_o)]^{-2}$ were used throughout the course of refinement. ^c The anisotropic temperature factor takes the form $\exp[-(\beta_{11}h^2 + \beta_{22}k^2 + \beta_{33}l^2 + 2\beta_{12}hk + 2\beta_{13}hl + 2\beta_{23}kl)]$. ^d The crystal used for data collection was bounded by the faces {011}, {01 $\bar{1}$ }, {011}, {0 $\bar{1}\bar{1}$ }, {100}, { $\bar{1}00$ }, and {102}. The perpendicular distances of these faces from the "origin" of the crystal were, respectively, 0.0076, 0.0076, 0.0074, 0.0074, 0.0162, 0.0162, and 0.0125 cm. The transmission factor (applied to $|F_o|$) ranged from 0.336 to 0.526.

scattering factors were taken from the compilation¹⁵ of Steart et al. A full account of the course of refinement is given in Table IV.

When calculated hydrogen atom coordinates were included in the scattering model as fixed contributions to $|F_c|$, the N-H and C-H distances were assumed to be 0.87 and 0.95 Å, respectively.¹⁶ The hydrogen atoms were assigned fixed isotropic temperature factors 10% greater than the equivalent isotropic temperature factors of the carbon or nitrogen atom to which they were bonded (i.e., $B_H = 1.1B_C$ Å²; $B_{NH} = 1.1B_N$ Å²). Hydrogen atom coordinates and temperature factors were recalculated prior to each refinement cycle, and no attempt was made to include the hydroxyl hydrogen atom in the scattering model.

On the final cycle of least-squares refinement, no individual parameter shift was greater than 0.15 of the corresponding parameter estimated standard deviation (estimated standard deviations are obtained from inversion of the block-diagonal matrices). A final electron density difference map showed no unusual features, and there were no residual peaks greater than 0.5 e/Å³. The standard deviation of an observation of unit weight, defined as $[\Sigma w(|F_o| - |F_c|)^2 / (m - n)]^{1/2}$ (where m is the number of observations and n (=199) is the number of parameters varied), is *cf.* 2.11, an expected value of 1.0 for ideal weighting. An examination of the final $|F_o|$ and $|F_c|$ values showed no evidence of serious extinction effects, and there is no serious dependence of the minimized function on either $|F_o|$ or $\lambda^{-1} \sin \theta$.

The final atomic positional and thermal parameters, together with their estimated standard deviations (where appropriate), are listed in Table V. A listing of observed and calculated structure factor amplitudes ($\times 10^4$) is available (for details regarding the availability of supplementary material, see the paragraph at the end of this paper).

Computer Programs. The data reduction and scaling program¹⁷ SETUP 3 and the program used for generation of $|E|$ values (EPROG) were written locally for the Univac-1108 computer (Whimp). The direct-methods package of programs (MULTAN) has been described previously.¹⁸ The sorting (SORTIF), Fourier (ANUFOR), and block-diagonal least-squares

(10) The formulae used for data reduction are as follows: LP (Lorentz-polarization factor) = $(\cos^2 2\theta + \cos^2 2\theta_m) / 2 \sin 2\theta$, where θ and θ_m (=13.25°) are the reflection and monochromator Bragg angles, respectively; I (net peak intensity) = $[CT - (t_p/t_b)(B_1 + B_2)]$, where CT is the total peak count in t_p (s) and B_1 and B_2 are the individual background counts in $(t_b/2)$ (s); $\sigma(I)$ (reflection significance) = $[CT + (t_p/t_b)^2(B_1 + B_2)]^{1/2}$; $\sigma(F_o)$ (the reflection esd) = $[\sigma(I)/LP]^2 + (\rho|F_o|^2)^2 / 2|F_o|$; $\sigma(F_c)$ (the reflection esd from counting statistics alone) = $\sigma(I) / 2(LP|F_o|)$; R_s (the statistical R factor) = $\Sigma \sigma(F_o) / \Sigma |F_o|$; background rejection ratio = $(|B_1 - B_2|) / (B_1 + B_2)^{1/2}$.

(11) (a) Busing, W. R.; Levy, H. A. *J. Chem. Phys.* **1957**, *26*, 563. (b) Corfield, P. W. R.; Doedens, R. J.; Ibers, J. A. *Inorg. Chem.* **1967**, *6*, 197.

(12) Cromer, D. T.; Mann, J. B. *Acta Crystallogr., Sect. A* **1968**, *A24*, 321.

(13) Prewitt, C. T. Ph.D. Thesis, Massachusetts Institute of Technology, 1962, p 163.

(14) Cromer, D. T.; Liberman, D. *J. Chem. Phys.* **1970**, *53*, 1891.

(15) Stewart, R. F.; Davidson, E. R.; Simpson, W. T. *J. Chem. Phys.* **1965**, *42*, 3175.

(16) Churchill, M. R. *Inorg. Chem.* **1973**, *12*, 1213.

(17) The program SETUP 3 corrects the intensity data for anisotropic crystal decomposition, according to the formula described by: Churchill, M. R.; Kalra, K. *Inorg. Chem.* **1974**, *13*, 1427.

(18) Germain, G.; Main, P.; Woolfson, M. M. *Acta Crystallogr., Sect. B* **1970**, *B26*, 274. *Acta Crystallogr., Sect. A* **1971**, *A27*, 368.

Table V. Fractional Atomic Positional and Thermal Parameters for [Co(trenenol)Cl]Br(ClO₄)

(a) Refined Positional and Anisotropic Thermal Parameters

ATOM	X/A	Y/B	Z/C	BETA11	BETA22	BETA33	BETA12	BETA13	BETA23
CO	0.462251121	0.20213181	0.37753151	0.007131161	0.00349171	0.00150131	-0.000221101	0.00055151	0.00003141
CL111	0.424841211	0.091501151	0.370821151	0.009171281	0.005971141	0.00366161	-0.001921161	0.001211111	-0.00049171
O111	1.0503171	0.1678151	0.4274131	0.01191101	0.0093151	0.0061131	0.0025161	-0.0019141	-0.0009131
N111	0.7379181	0.1251151	0.4706131	0.01781141	0.0063151	0.0030121	-0.0005171	0.0003141	0.00015131
N121	0.5829171	0.3286151	0.4392131	0.01191111	0.0054151	0.0020121	0.0003161	0.0018131	-0.0004121
N131	0.8593171	0.2980141	0.3062131	0.03951101	0.0045141	0.0025121	-0.0010151	0.0011131	0.0000121
N141	0.7791171	0.0806151	0.3251131	0.01181111	0.0042141	0.0032121	-0.0009161	0.0013141	-0.0006121
N151	0.5672171	0.2752151	0.2886131	0.01241111	0.0066151	0.0019121	-0.0004161	-0.0008141	0.0000121
C111	0.69121131	0.1977111	0.5349141	0.03201241	0.0093181	0.0016121	-0.00391121	0.0007161	0.0005131
C121	0.55041111	0.2753171	0.5110141	0.02281201	0.0078181	0.0026131	-0.00361101	0.0039161	-0.0003131
C131	0.71071101	0.4274161	0.4447141	0.01531141	0.0051161	0.0023121	-0.0011171	0.0015151	-0.0008131
C141	0.8781191	0.3811161	0.4311141	0.01421141	0.0057161	0.0021121	-0.0021171	0.0000141	-0.0007131
C151	1.0373191	0.2180161	0.3588141	0.00781121	0.0068161	0.0043131	0.0009171	0.0016151	-0.0001131
C161	0.94771101	0.1190161	0.3074151	0.01521161	0.0053161	0.0053141	0.0009181	0.0044161	-0.0012141
C171	0.8311101	0.3742161	0.2979141	0.01831161	0.0068161	0.0018121	-0.0007181	0.0017151	0.0007131
C181	0.69801111	0.3235171	0.2463141	0.02261181	0.007171	0.0042121	-0.0005191	0.0021151	0.0007131
BR	0.699951131	-0.007271181	0.13425151	0.019161191	0.01025191	0.00400131	-0.002721111	-0.00053161	0.00022141
CL121	0.183451241	0.262041151	0.129761101	0.013991331	0.00660141	0.00328161	-0.001711161	0.001421111	-0.00108181
O1211	0.04611111	0.3167171	0.1573151	0.03241201	0.0154191	0.0113151	-0.00011121	0.0101161	-0.0007141
O1221	0.14231101	0.1821161	0.0742141	0.03871211	0.0099161	0.0069131	-0.00301101	-0.0077171	-0.0037141
O1231	0.29421161	0.3308181	0.1126161	0.08531421	0.0133191	0.0170171	-0.01921161	0.03161151	-0.0099171
O1241	0.25001151	0.19131101	0.1855151	0.05781341	0.02661151	0.0079141	0.00661201	-0.01101101	-0.0018171

(b) Calculated Hydrogen Atom Coordinates and Fixed Isotropic Temperature Factors^a

ATOM	X/A	Y/B	Z/C	B1A**21	ATOM	X/A	Y/B	Z/C	B1A**21
HN11A1	0.846	0.117	0.473	4.3	H13A1	0.714	0.461	0.492	3.5
HN11B1	0.692	0.035	0.472	4.3	H13B1	0.679	0.487	0.410	3.5
HN121	0.490	0.360	0.421	3.1	H14A1	0.950	0.445	0.421	3.5
HN14A1	0.720	0.064	0.285	3.4	H14B1	0.924	0.339	0.472	3.5
HN14B1	0.789	0.017	0.352	3.4	H151	1.099	0.260	0.342	4.1
HN15A1	0.501	0.333	0.299	3.4	H16A1	0.943	0.147	0.259	4.9
HN15B1	0.511	0.222	0.263	3.4	H16B1	1.023	0.054	0.313	4.9
H11A1	0.784	0.245	0.593	5.5	H17A1	0.933	0.378	0.275	3.9
H11B1	0.659	0.146	0.572	5.5	H17B1	0.799	0.492	0.311	3.9
H12A1	0.450	0.230	0.506	4.9	H18A1	0.653	0.384	0.215	4.5
H12B1	0.540	0.337	0.546	4.9	H18B1	0.743	0.262	0.218	4.5

^a The hydrogen atoms are numbered according to the nitrogen [NH(*n*)] or carbon [H(*n*)] atom to which they are bonded.

refinement (BLKLSQ) programs have been described previously.¹⁹ Absorption corrections were carried out by using TOMPAB, a locally modified version (J. D. Bell) of the Brookhaven National Laboratory absorption correction program.²⁰ The figures were produced by using ORTEP,²¹ while bond lengths and interbond angles, together with their estimated standard deviations, were calculated by using ORTEP.²² These programs are packaged in ANUCRYS, and the calculations were carried out on a Univac-1108 computer.

Results

Characterization of Reactants and Products. The new ions [Co(NH₃)₅NH₂CH₂CH(OH)CH₃]³⁺, [Co(NH₃)₅NH₂CH₂COCH₃]³⁺, [Co(NH₃)₄(NH₂CH₂C(OH)(CH₃)NH₂)]³⁺, [Co(NH₃)₅NH₂CH₂CH(OH)C₆H₅]³⁺, and [Co(NH₃)₅NH₂CH₂COC₆H₅]³⁺ have been synthesized and all exhibit absorption maxima in the range 470–480 nm that are typical of complexes of the CoN₆³⁺ chromophore where N is a saturated amine. The coordinated imines [Co(NH₃)₄(NH₂CH₂C(CH₃)=NH)]³⁺, [Co(NH₃)₄(NH=C(CH₃)C(CH₂OH)₂NH₂)]³⁺, however, show absorption maxima at significantly higher energies than those above consistent with the presence of imine groups. In particular, the absorption maxima of [Co(NH₃)₃(HN=C(CH₃)CH₂CH₂N=C(CH₃)CH₂NH₂)]³⁺ (λ_{max} 451 nm) moved to even shorter wavelengths consistent with the presence of two imine groups in this complex. Similar shifts to higher energy were

observed^{2a} when [Co(NH₃)₅O₂CCOCH₃]²⁺ (λ_{max} 500 nm) cyclized to [Co(NH₃)₄O₂C(CH₃)=NH]²⁺ (λ_{max} 483 nm). The new imine complexes are also characterized by the resonance due to HN=C which occurs at δ 10–11 in the ¹H NMR spectra.

The ions [Co(trien)(NH₂CH₂CH(OH)₂)Cl]²⁺ and [Co(trien)(NH₂CH₂CH(OCH₃)₂)Cl]²⁺ are assigned the α configuration³ from the similarity of their absorption spectra and ¹H NMR spectra (Figure 1) to those of complexes of known configuration:^{23,24} α-[Co(trien)(NH₃)Cl]²⁺ 530 nm (ε = 95 M⁻¹ cm⁻¹), β₂-[Co(trien)(NH₃)Cl]²⁺ 475 (93), β₂'-[Co(trien)(NH₃)Cl]²⁺ 475 (84), [Co(trien)(NH₂CH₂CH(OH)₂)Cl]²⁺ 534 (106), 367 (106), [Co(trien)(NH₂CH₂CH(OCH₃)₂)Cl]²⁺ 535 (105), 367 (102).

The ¹H NMR spectra of the [Co(trien)(NH₂CH₂CHO)Cl]²⁺, [Co(trien)(NH₂CH₂CH(OH)₂)Cl]²⁺, and α-[Co(trien)(NH₃)Cl]²⁺ ions,²³ excluding resonances due to the coordinated aminoacetaldehyde, gem-diol, and ammine ligands, respectively, are almost identical, and the relative proton-exchange rates are similar.

The ion [Co(trenenol)Cl]²⁺, generated from near neutral solutions of [Co(trien)(NH₂CH₂CH(OH)₂)Cl]²⁺, and its derivative [Co(trenenone)Cl]²⁺ can be assigned the *t* configuration from the similarity of their visible absorption maxima to those of related complexes of known configurations (*t*-[Co(trenenol)Cl]²⁺ 530 nm (ε 151), 362 (133), *t*-[Co(trenenol)(NH₃)Cl]²⁺ 530 (136), 363 (126), *s*-[Co(trenenol)Cl]²⁺ 512 (151), [Co(trenenone)Cl]²⁺ 531 (147), 361 (137), [Co(trenenone)Cl]²⁺ 532 (137), 362 (129)). The new complexes exhibit absorption maxima near 530 nm typical of *t* isomers whereas the *s* isomers show maxima near 512 nm.^{25,26}

(19) Robertson, G. B.; Whimp, P. O. *Inorg. Chem.* **1974**, *13*, 1047.

(20) The analytical method used for calculating transmission factors is described by: De Meulenaer, J.; Tompa, H. *Acta Crystallogr.* **1965**, *19*, 1014; Alcock, N. W. *Acta Crystallogr., Sect. A* **1969**, *A25*, 518.

(21) Johnson, C. K. Report ORNL-3794; Oak Ridge National Laboratory: Oak Ridge, Tenn., 1965.

(22) Busing, W. R.; Martin, K. O.; Levy, H. A. Report ORNL-TM-306; Oak Ridge National Laboratory: Oak Ridge, Tenn., 1964.

(23) Dwyer, M. Ph.D. Thesis, Australian National University, 1971.

(24) Buckingham, D. A.; Foster, D. M.; Marzilli, L. G.; Sargeson, A. M. *Inorg. Chem.* **1970**, *9*, 11. Dwyer, M.; Maxwell, I. E. *Ibid.* **1970**, *9*, 1459.

(25) Cresswell, P. J. Ph.D. Thesis, Australian National University, 1974.

Table VI. Bond Lengths and Interbond Angles

(a) Bond Lengths, Å					
atoms	distance	atoms	distance	atoms	distance
Co-Cl(1)	2.273 (3)	Co-N(1)	1.979 (6)	Co-N(2)	1.957 (5)
Co-N(3)	1.935 (5)	Co-N(4)	1.953 (6)	Co-N(5)	1.942 (5)
N(1)-C(1)	1.511 (10)	C(1)-C(2)	1.466 (12)	C(2)-N(2)	1.497 (9)
N(2)-C(3)	1.507 (9)	C(3)-C(4)	1.477 (11)	C(4)-N(3)	1.518 (8)
N(3)-C(5)	1.502 (9)	C(5)-C(6)	1.516 (11)	C(6)-N(4)	1.477 (10)
N(3)-C(7)	1.529 (8)	C(7)-C(8)	1.490 (11)	C(8)-N(5)	1.457 (10)
C(5)-O(1)	1.416 (10)				
Cl(2)-O(21)	1.389 (9)	Cl(2)-O(22)	1.386 (7)	Cl(2)-O(23)	1.331 (11)
Cl(2)-O(24)	1.390 (11)				

(b) Interbond Angles, Deg					
atoms	angle	atoms	angle	atoms	angle
Cl(1)-Co-N(1)	87.4 (2)	Cl(1)-Co-N(2)	94.7 (2)	Cl(1)-Co-N(3)	174.3 (2)
Cl(1)-Co-N(4)	93.2 (2)	Cl(1)-Co-N(5)	88.0 (2)	N(1)-Co-N(2)	84.4 (2)
N(1)-Co-N(3)	97.9 (2)	N(1)-Co-N(4)	90.0 (2)	N(1)-Co-N(5)	174.8 (3)
N(2)-Co-N(3)	87.8 (2)	N(2)-Co-N(4)	170.1 (4)	N(2)-Co-N(5)	93.6 (2)
N(3)-Co-N(4)	84.8 (2)	N(3)-Co-N(5)	86.8 (2)	N(4)-Co-N(5)	92.7 (2)
Co-N(1)-C(1)	111.7 (5)	Co-N(2)-C(2)	108.2 (4)	Co-N(2)-C(3)	109.0 (4)
Co-N(3)-C(4)	106.9 (4)	Co-N(3)-C(5)	109.4 (4)	Co-N(3)-C(7)	109.2 (4)
Co-N(4)-C(6)	112.7 (4)	Co-N(5)-C(8)	111.1 (4)	N(1)-C(1)-C(2)	108.3 (6)
C(1)-C(2)-N(2)	108.9 (7)	C(2)-N(2)-C(3)	113.3 (5)	N(2)-C(3)-C(4)	110.5 (5)
C(3)-C(4)-N(3)	108.2 (5)	C(4)-N(3)-C(5)	114.0 (5)	C(4)-N(3)-C(7)	108.0 (5)
C(5)-N(3)-C(7)	109.1 (5)	N(3)-C(5)-C(6)	106.4 (6)	N(3)-C(5)-O(1)	108.6 (6)
O(1)-C(5)-C(6)	108.7 (6)	C(5)-C(6)-N(4)	109.0 (6)	N(3)-C(7)-C(8)	111.7 (6)
C(7)-C(8)-N(5)	107.9 (6)				
O(21)-Cl(2)-O(22)	114.0 (5)	O(21)-Cl(2)-O(23)	110.0 (6)	O(21)-Cl(2)-O(24)	105.9 (6)
O(22)-Cl(2)-O(23)	113.3 (6)	O(22)-Cl(2)-O(24)	104.0 (5)	O(23)-Cl(2)-O(24)	109.0 (7)

Table VII. Selected Least-Squares Planes

(a) Best Weighted Least-Squares Planes					
plane	atoms defining plane	equation ^a			
1	Co, Cl(1), N(2), N(3), N(4)	$-0.3107X + 0.4467Y - 0.8390Z + 6.3108 = 0$			
2	Co, N(1), N(2)	$0.8870X + 0.4616Y - 0.0146Z - 5.1890 = 0$			
3	Co, N(2), N(3)	$-0.4017X + 0.4392Y - 0.8035Z + 6.5188 = 0$			
4	Co, N(3), N(4)	$-0.3523X + 0.3539Y - 0.8664Z + 6.9135 = 0$			
5	Co, N(3), N(5)	$0.4253X - 0.7324Y - 0.5318Z + 3.3295 = 0$			

(b) Deviations (Å) of Atoms from Planes					
atom	plane 1	atom	plane 1	atom	plane 2
Co	-0.0028 (9)	N(1)	-1.977 (6)	Co	0.000 (1)
Cl(1)	0.014 (2)	N(5)	1.938 (5)	N(1)	0.000 (7)
N(2)	-0.098 (5)	C(3)	-0.003 (7)	N(2)	0.000 (6)
N(3)	0.158 (5)	C(4)	-0.448 (7)	C(1)	-0.052 (10)
N(4)	-0.114 (6)	C(5)	-0.500 (8)	C(2)	-0.614 (9)
		C(6)	-0.076 (8)	C(3)	1.411 (7)

atom	plane 3	atom	plane 4	atom	plane 5
Co	0.000 (1)	Co	0.000 (1)	Co	0.000 (1)
N(2)	0.000 (5)	N(3)	0.000 (5)	N(3)	0.000 (5)
N(3)	0.000 (5)	N(4)	0.000 (6)	N(5)	0.000 (6)
C(2)	-0.183 (8)	C(4)	-0.728 (7)	Cl(1)	0.088 (2)
C(3)	-0.002 (7)	C(5)	-0.621 (8)	N(1)	-0.076 (6)
C(4)	-0.576 (7)	C(6)	-0.050 (9)	C(7)	-0.012 (7)
C(5)	-0.765 (8)			C(8)	0.488 (8)

^a The plane equations $LX + MY + NZ + D = 0$ refer to orthogonal coordinates where $X = 8.0092x + 0.0y - 1.3787z$, $Y = 0.0x + 11.2275y + 0.0z$, and $Z = 0.0x + 0.0y + 18.4396z$.

The ¹H NMR spectra of the complexes show a broad secondary amine proton resonance (*cis* to coordinated Cl⁻) at δ 6.60 and 6.50, which is near the position of the corresponding signal in the

Table VIII. Torsion Angles

atom 1	atom 2	atom 3	atom 4	torsion angle, ^a deg
N(1)	C(1)	C(2)	N(2)	-43.3 (8)
N(2)	C(3)	C(4)	N(3)	43.9 (7)
N(3)	C(5)	C(6)	N(4)	-41.6 (7)
N(3)	C(7)	C(8)	N(5)	37.9 (8)

^a The torsion angle is positive if, when looking from atom 2 to atom 3, a clockwise motion of atom 1 superimposes it on atom 4.

reactive aminoacetaldehyde complex (δ 6.48). Also *N*-deuterated [Co(trenenol)Cl]²⁺ displays a sharp doublet (δ 4.36, 4.39) and a triplet (δ 5.28, 5.36, 5.44) arising from spin-spin splitting between the methylene group and >CH(OD) on the carbinolamine moiety (Figure 2C). The sharpness of these resonances indicates the presence of only one configuration of the carbinolamine function. On oxidation to the trenenone complex, the doublet disappeared and was replaced by a triplet (δ 5.20, 5.29, 5.38) which collapsed to a singlet on *N*-deuteration. There is no indication in the ¹H NMR spectra or the visible absorption spectra that elimination of water from the carbinolamine has occurred to yield an imine.

At this point the condensation is consistent with either addition of the carbonyl function at a *secondary* amine center or with addition at one of the *primary* amine centers, provided that steric considerations restrict the dehydration. A crystal structure determination was carried out to resolve this question.

Structure of [Co(trenenol)Cl]²⁺. Crystals of [Co(trenenol)-Cl]Br(ClO₄) contain equal quantities of (SSS)-[Co(trenenol)Cl]²⁺ and (RRR)-[Co(trenenol)Cl]²⁺ cations, together with bromide and perchlorate anions. Neither the complex cation nor the perchlorate anion has crystallographic or virtual symmetry higher than C₁. The coordination at the central cobalt atom of the cation is essentially octahedral, with five coordination sites being occupied by the trenenol, 3-(2-amino-1-hydroxyethyl)-1,8-diamino-3,6-diazaoctane, ligand; the sixth coordination site is occupied by a chlorine atom. In addition, the complex cation has chiral centers at N(2), N(3), and C(5). A perspective view of the (SSS)-[Co(trenenol)Cl]²⁺ cation is shown in Figure 3 while the contents of one unit cell are shown by the stereopairs in Figure 4. In both figures, the thermal ellipsoids have been drawn to include 50%

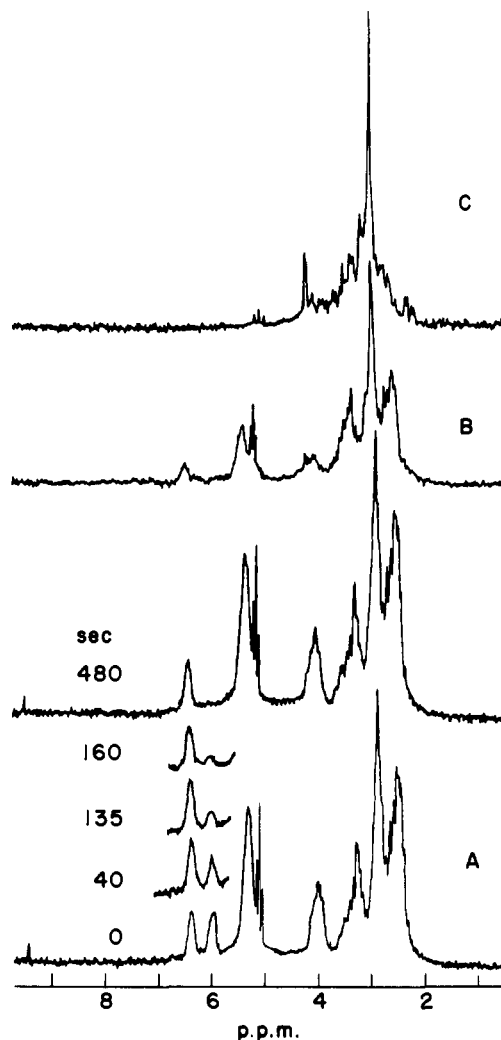


Figure 2. (A) Proton-exchange reaction of $(RR,SS)\text{-}\alpha\text{-}[\text{Co}(\text{trien})\text{-(NH}_2\text{CH}_2\text{CHO)Cl}]\text{Br}_2\cdot 2\text{H}_2\text{O}$ in D_2O (pD 4.9): k_{obsd} (32 °C) = $1.2 \times 10^8 \text{ M}^{-1} \text{ s}^{-1}$ for secondary N-H resonance at 6.08 ppm. (B) Condensation in 0.25 M pyridine/pyridinium buffer (pD 4.9). For clarity, the peaks due to pyridine and pyridinium ion have been removed. (C) *N*-deuterated $(RRR,SSS)\text{-}t\text{-}[\text{Co}(\text{trenenol)Cl}]\text{Br}(\text{ClO}_4)$ in D_2O (reference sodium (trimethylsilyl)propanesulfonate).

of the probability distribution and, for clarity, all but one of the hydrogen atoms have been omitted.

Principal bond distances and interbond angles, together with their estimated standard deviations, are shown in Table VI. The results of weighted least-squares planes calculations are listed in Table VII,²⁷ while torsion angles within the five-coordinated trenenol ligand are collected in Table VIII.

The Co-Cl distance [Co-Cl(1) = 2.273 (3) Å] is typical and lies within the range of other recent determinations, e.g., 2.237 (4) Å for $\beta\text{-}[\text{Co}(\text{trien})(\text{H}_2\text{O})\text{Cl}]^{2+}$,²⁸ 2.286 (2) Å for $[\text{Co}(\text{N-H}_3)_5\text{Cl}]\text{Cl}_2$,²⁹ and 2.303 (6) Å for $[\text{Co}(\text{NH}_3)_5\text{Cl}]\text{SiF}_6$.³⁰ In the very closely related derivative $[\text{Co}(\text{Metrenen})\text{Cl}]^{2+}$ (Metrenen = 3-(2-aminoethyl)-6-methyl-1,8-diamino-3,6-diazaoctane), the corresponding distance is 2.248 (5) Å.³¹

The Co-N distances range from 1.935 (5) [Co-N(3)] to 1.979 (6) Å [Co-N(1)] ($\Delta = 0.044$ Å; $\Delta/\sigma \approx 8$) and average 1.953 Å. Similar average Co-N distances have been observed for $\beta\text{-}[\text{Co}(\text{trien})(\text{H}_2\text{O})\text{Cl}]^{2+}$ (1.93 Å)²⁸ and $[\text{Co}(\text{en})_2(\text{CH}_3\text{NHCH}_2\text{CO}_2)]^{2+}$

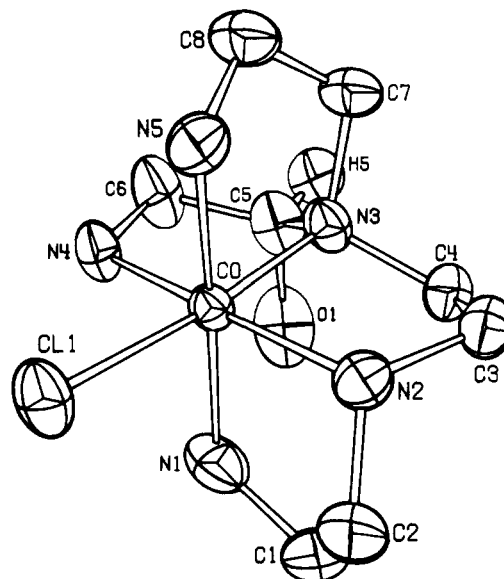


Figure 3. The stereochemistry of the cation, $(SSS)\text{-}t\text{-}[\text{Co}(\text{trenenol)Cl}]^{2+}$, showing the atom-numbering scheme.

(1.97 Å)³² and 1.963 Å has been observed for $\Delta\text{-}\beta_1\text{-}RR\text{-}[\text{Co}(\text{trien})(\text{gly})]^{2+}$ ²³ and 1.951 Å for $\Delta\text{-}\beta_1\text{-}RS\text{-}[\text{Co}(\text{trien})(\text{gly})]^{2+}$.³³ In the $[\text{Co}(\text{Metrenen})\text{Cl}]^{2+}$ cation, the five Co-N distances range from 1.923 (11) to 2.027 (16) Å, with an average value of 1.97 Å.³¹

As the N-Co-N angles within each five-atom chelate ring are all less than 90° (average 86.0°), the coordination at the central cobalt atom is not precisely octahedral; similar results have been observed for other cobalt(III)-amine chelate derivatives; e.g., for $[\text{Co}(\text{trien})(\text{H}_2\text{O})\text{Cl}]^{2+}$, the average N-Co-N angle is 86.4°.²⁸ The five-atom chelate ring defined by Co, N(3), N(5), C(7), C(8) has an asymmetrical skew conformation; C(7) is -0.012 (7) Å from the plane of Co, N(3), and N(5), while C(8) is 0.488 (3) Å from this plane. The three remaining five-atom chelate rings have the asymmetrical envelope configuration in which the two carbon atoms are on the same side of the N-Co-N plane.

Within the five-coordinate trenenol ligand, the N-C distances average 1.500 Å, while the C-C distances average 1.487 Å.

The bond C(5)-O(1) [1.416 (10) Å] is a simple σ bond and as such is in excellent agreement with the value of 1.426 (5) Å normally expected for carbon-oxygen single bonds.³⁴ Unfortunately, it was not possible to locate the hydrogen atom bonded to O(1), but it is interesting to note that O(1) is axially bonded to C(5). This, in turn, gives rise to an extremely short O-H contact [O(1)-HN(1A)] of 2.01 Å [O(1)-HN(1A)-N(1) angle = 144.2°]³⁵ which is indicative of a strong hydrogen bond [the distance O(1)-N(1) is 2.762 (9) Å, while the sum of the van der Waals contact distance for O and N is 2.9 Å].³⁶

Amine-Proton Exchange. The ^1H NMR spectrum of $[\text{Co}(\text{N-H}_3)_5\text{NH}_2\text{CH}_2\text{COCH}_3](\text{ClO}_4)_3$ exhibits 2 broad resonances at δ 3.6 and 4.4 (15 and 2 protons, respectively) which are typical of $^1\text{H}\text{-}^{14}\text{N}\text{-}^{59}\text{Co}$ coupling. When this spectrum is compared with that³⁷ of $[\text{Co}(\text{NH}_3)_5\text{NCCH}_3]^{3+}$, the resonance at δ 3.6 is assigned to undifferentiated cis and trans NH_3 and the two proton resonance at δ 4.4 is assigned to the aminoacetone NH_2 moiety. The time-dependent change of the spectrum of $[\text{Co}(\text{NH}_3)_5\text{NH}_2\text{C-}$

(27) The method used for calculating weighted least-squares planes is described by: Blow, D. M. *Acta Crystallogr.* **1960**, *13*, 168.

(28) Freeman, H. C.; Maxwell, I. E. *Inorg. Chem.* **1969**, *8*, 1293.

(29) Messmer, G. G.; Amma, E. L. *Acta Crystallogr., Sect. B* **1968**, *B24*, 417.

(30) Stanko, J. A.; Paul, I. C. *Inorg. Chem.* **1967**, *6*, 486.

(31) Buckingham, D. A.; Dwyer, M.; Sargeson, A. M.; Watson, K. J. *Acta Chem. Scand.* **1972**, *26*, 2813.

(32) Blount, J. F.; Freeman, H. C.; Sargeson, A. M.; Turnbull, K. R. *Chem. Commun.* **1967**, 324.

(33) Buckingham, D. A.; Cresswell, P. J.; Dellaca, R. J.; Dwyer, M.; Gainsford, G. J.; Marzilli, L. G.; Maxwell, I. E.; Robinson, W. T.; Sargeson, A. M.; Turnbull, K. R. *J. Am. Chem. Soc.* **1974**, *96*, 1713.

(34) *Chem. Soc. Spec. Publ.* **1964**, No. 18, 520s.

(35) The N-H distances have been set at 0.87 Å (the "X-ray" bond length), whereas the true internuclear separation should be ca. 1.01 Å. The true O(1)-HN(1A) distance is ca. 1.90 Å.

(36) Hamilton, W. C.; Ibers, J. A. "Hydrogen Bonding in Solids"; W. A. Benjamin Inc., New York, 1968; p 16.

(37) Buckingham, D. A.; Keene, F. R.; Sargeson, A. M. *J. Am. Chem. Soc.* **1973**, *95*, 5649.

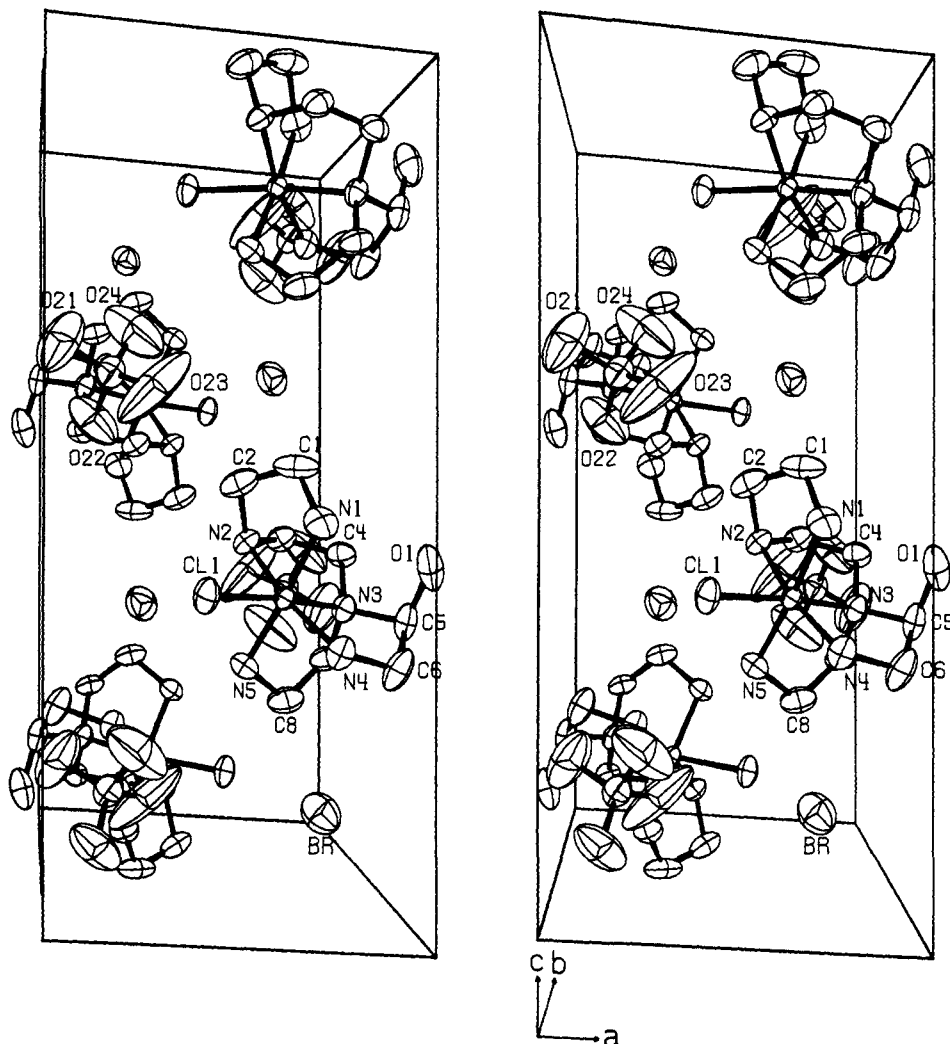


Figure 4. Contents of one unit cell.

$\text{H}_2\text{COCH}_3](\text{ClO}_4)_3$ in pyrazole/DCl buffers indicates that the coordinated ammine protons exchange at a rate ($k_{\text{OD}} = 3.0 \times 10^6 \text{ M}^{-1} \text{ s}^{-1}$ assuming $\text{p}K_{\text{D}_2\text{O}} = 14.18$ at $\mu = 1.0$ and 25°C) which is about tenfold less than the exchange of the aminoacetone amine protons.

The ^1H NMR spectrum of $(RR,SS)\text{-}\alpha\text{-}[\text{Co}(\text{trien})\text{Cl}(\text{NH}_2\text{CH}_2\text{CHO})]\text{Br}_2 \cdot 2\text{H}_2\text{O}$ (Figure 2A) exhibits four broad resonances at δ 4.16, 5.30, 6.08, and 6.48 (2, 4, 1, and 1 protons, respectively). When this spectrum is compared with that of $\alpha\text{-}[\text{Co}(\text{trien})(\text{NH}_3)\text{Cl}]^{2+}$, the resonance at δ 4.16, which does not appear in the latter spectrum, can be assigned to the $-\text{NH}_2$ of the aminoacetaldehyde/*gem*-diol ligand. The mutually trans primary amine protons are assigned to the resonance at δ 5.30. With use of the collected data for the *N*-proton resonances of polyaminecobalt(III) complexes,^{23,26} the resonances at δ 6.08 and 6.48 are assigned to the secondary amine protons trans and cis to the coordinated chloride, respectively. The change of the spectrum of $(RR,SS)\text{-}\alpha\text{-}[\text{Co}(\text{trien})(\text{NH}_2\text{CH}_2\text{CHO})\text{Cl}]\text{Br}_2 \cdot 2\text{H}_2\text{O}$ in D_2O with time (Figure 2A) then indicates that the secondary amine proton trans to the coordinated chloride exchanges at a rate ($k_{\text{OD}} = 1.2 \times 10^8 \text{ M}^{-1} \text{ s}^{-1}$, $\text{p}K_{\text{D}_2\text{O}} = 14.0$, $\mu = 1$, 32°C) which is about 30-fold faster than the rate of exchange of the secondary amine proton cis to the chloride. This analysis assumes an activation energy of 29 kcal/mol for proton exchange.³⁸ After 20 h at 25°C , the spectrum broadened considerably. This was ascribed to the generation of some Co(II) species. Ion-exchange chromatography of the sample at this point showed the presence of violet $2+$ and orange $3+$ Co(III) species as well as some

polymeric material and some Co^{2+} .

Methyl and Methylene-Proton Exchange. The ^1H NMR spectrum of $[\text{Co}(\text{NH}_3)_4(\text{NH}=\text{C}(\text{CH}_3)\text{CH}_2\text{NH}_2)](\text{ClO}_4)_3$ in $\text{Na}_2\text{CO}_3/\text{NaHCO}_3$ buffer (pH 10.56) exhibited two sharp resonances at δ 4.03 ($-\text{CH}_2-$) and 2.37 ($-\text{CH}_3$); all amine protons were exchanged rapidly under these conditions. The change of this spectrum with time indicated that the methylene protons exchanged at a rate ($k_{\text{OD}} = 13.5 \text{ M}^{-1} \text{ s}^{-1}$, $\text{p}K_{\text{D}_2\text{O}} = 14.29$, $\mu = 0.5$, 25°C) which was much faster than the rate of exchange of the methyl protons under the same conditions ($k_{\text{OD}} = 5.4 \times 10^{-2} \text{ M}^{-1} \text{ s}^{-1}$). After 60 h at 25°C , the spectrum broadened considerably due to the generation of some Co(II) species.

Kinetics of Condensation. In the pH range 3.6–7.5, whether controlled by pH-stat or by buffers, two consecutive reactions were observed for the base-catalyzed cyclization of $[\text{Co}(\text{NH}_3)_5\text{NH}_2\text{C}(\text{H}_2\text{COCH}_3)](\text{ClO}_4)_3$. Also, the ^1H NMR and visible spectra of the final product (after 10 half-lives of the slower reaction process) were identical with those of the $[\text{Co}(\text{NH}_3)_4(\text{NH}_2\text{CH}_2\text{C}(\text{CH}_3)=\text{NH})]^{3+}$ ion. ^1H NMR spectroscopy showed that the reactant complex was in the ketone (nonhydrated) form; the hydrated form (*gem*-diol) was not detected. During the consecutive reactions, the ketone methyl resonance (δ 2.18) vanished and was replaced by an upfield carbinolamine resonance (δ 1.65) which in turn decayed to give the final imine-methyl resonance (δ 2.37). Estimates of the rate by this method agreed well with the spectral measurements.

During the processes, the visible absorption spectrum changed from that of the initial ketone complex (λ_{max} 478 nm) to that of the $[\text{Co}(\text{NH}_3)_4(\text{NH}_2\text{CH}_2\text{C}(\text{CH}_3)(\text{OH})\text{NH}_2)]^{3+}$ complex (λ_{max} 471 nm) with a marked decrease in absorbance in the 290-nm region and a small increase at 470 nm. Subsequently, a marked

(38) Buckingham, D. A.; Marzilli, L. G.; Sargeson, A. M. *Inorg. Chem.* 1968, 7, 915.

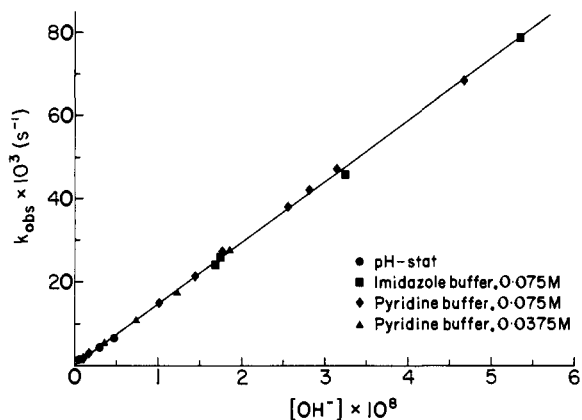


Figure 5. Kinetic data for the base-catalyzed condensation of $[\text{Co}(\text{NH}_3)_5(\text{NH}_2\text{CH}_2\text{COCH}_3)]^{3+}$ ion to $[(\text{NH}_3)_4\text{CoNH}_2\text{CH}_2\text{C}(\text{OH})(\text{CH}_3)\text{-NH}_2]^{3+}$ ion at 25 °C ($\mu = 1.0$). See Supplementary data for details.

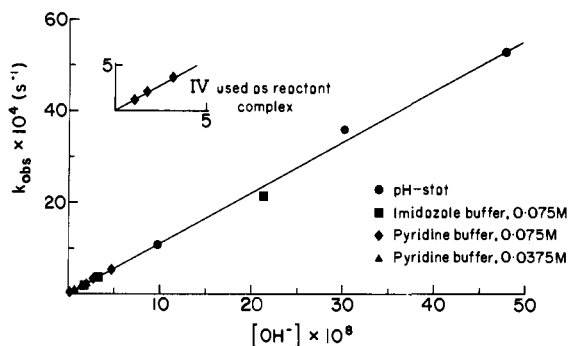


Figure 6. Kinetic data for the conversion of $[\text{Co}(\text{NH}_3)_4(\text{NH}_2\text{CH}_2\text{C}(\text{OH})(\text{CH}_3)\text{NH}_2)]^{3+}$ ion to $[\text{Co}(\text{NH}_3)_4(\text{HN}=\text{C}(\text{CH}_3)\text{CH}_2\text{NH}_2)]^{3+}$ ion at 25 °C ($\mu = 1.0$). See Supplementary data for details.

increase in absorbance in the 460- and 335-nm regions was observed, and the final spectrum ($\lambda_{\text{max}} 465 \text{ nm}$) corresponded to that of the $[\text{Co}(\text{NH}_3)_4(\text{NH}_2\text{CH}_2\text{C}(\text{CH}_3)=\text{NH})]^{3+}$ complex.

The spectrophotometric changes at 290 and 335 nm for carbinolamine and imine production, respectively, gave linear plots of $\log [(A_\infty - A)]$ against time for at least 5 half-lives. The reactions were followed under pseudo-first-order conditions and $k_{\text{obs}} = k[\text{OH}^-]$ for both processes. The plots of k_{obs} vs. $[\text{OH}^-]$ for both reactions (Figures 5 and 6) are linear. The rate constant for the first process, carbinolamine formation, k_c , is $1.47 (\pm 0.11) \times 10^6 \text{ M}^{-1} \text{ s}^{-1}$. The second process, imine formation, is slower with a rate constant k_i of $1.12 (\pm 0.15) \times 10^4 \text{ M}^{-1} \text{ s}^{-1}$. Imine formation was observed by using both the parent complex and the isolated carbinolamine complex (Figure 6). Identical rates were obtained from both sources, and the first process observed therefore must be carbinolamine formation.

In Figures 5 and 6, it can be seen that there is no dependence of rate constants on buffer concentration or buffer pK_a for pyridine and imidazole. However, when acetate is used as buffer, although the same rate law is observed, the rate constant for carbinolamine formation ($1.22 (\pm 0.06) \times 10^6 \text{ M}^{-1} \text{ s}^{-1}$) is measurably less than the value obtained under the former conditions. The difference is not great, and we cannot see much significance in the result. It could be ascribed to ion association between the 3+ cation and acetate ion for example.

In contrast to the consecutive reactions observed above, over the pH range 5.0–7.5, $(RR,SS)\text{-}\alpha\text{-}[\text{Co}(\text{trien})(\text{NH}_2\text{CH}_2\text{CHO})\text{-Cl}]\text{Br}_2\text{H}_2\text{O}$ displays only one reaction, formation of carbinolamine (Figure 2B). No evidence for mixtures of products was obtained from ion-exchange chromatography of the product. Also, the ^1H NMR and visible spectra of products isolated from the different types of kinetic experiments were identical with those of the much larger synthetic sample. Finally, base hydrolysis of the Cl^- ion and reanation of the product with Cl^- regenerates the same product.

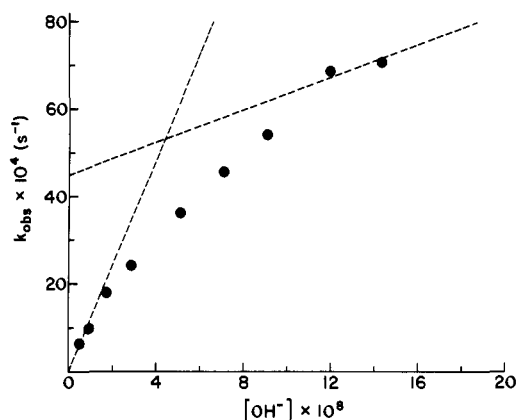


Figure 7. Kinetic data for the base catalyzed condensation of $(RR,SS)\text{-}\alpha\text{-}[\text{Co}(\text{trien})(\text{NH}_2\text{CH}_2\text{CHO})\text{Cl}]^{2+}$ ion.

Base hydrolysis of coordinated chloride ion was observable above pH 7.5, but at pH < 7.5 it was slow ($>10^4$ -fold slower than the rate of condensation) and did not complicate the measurement of the condensation kinetics. ^1H NMR spectroscopy (Figure 1C) showed that the reactant complex in solution was largely in the *gem*-diol form ($\sim 90\%$) with only a small fraction of free aldehyde present ($\sim 10\%$). During the reaction, the aldehyde resonance ($\delta 9.67$) vanished and a triplet grew at $\delta 5.28, 5.36$, and 5.44 consistent with the production of carbinolamine.

Some Co(II) was generated slowly in the concentrated solution ^1H NMR experiments, and this interfered with the rate measurements by this technique. However, estimates of the rate by this method agreed roughly with the spectral measurements.

During the reaction the visible absorption spectrum changed from that of the initial free aldehyde/*gem*-diol mixture ($\lambda_{\text{max}} 534 \text{ nm}$) to that of the trenenol complex ($\lambda_{\text{max}} 531 \text{ nm}$) with a marked increase in absorbance (A) in the 360- and 530-nm regions. This type of change is not consistent with imine formation where a marked shift of the first ligand field band to shorter wavelength would be expected.^{2c} The spectrophotometric rates obtained at 530 and 360 nm agreed and gave linear plots of $\log (A_\infty - A)$ against time for at least 4–5 half-lives.

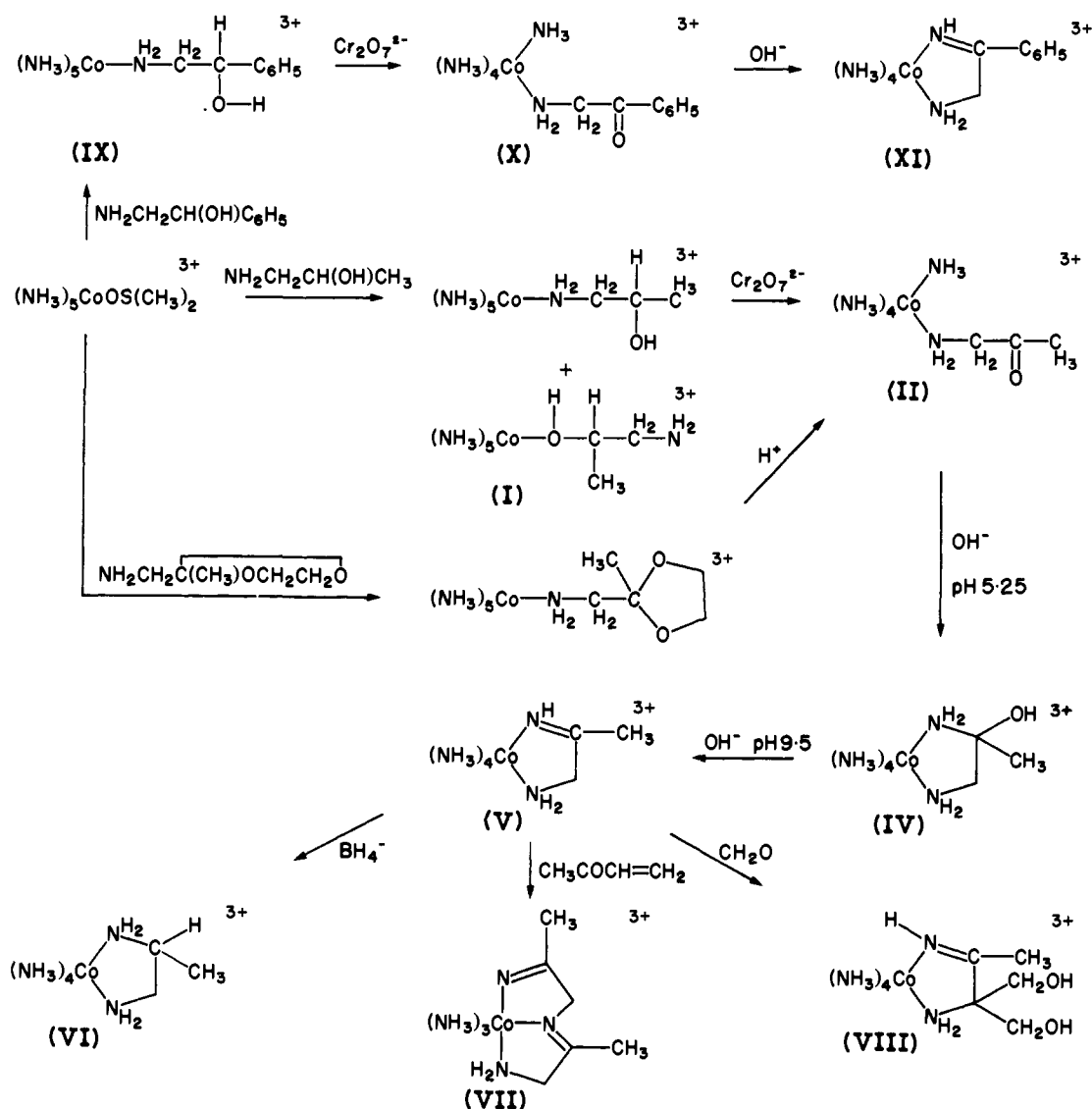
The results of the pH-stat experiments (Figure 7) are strikingly different from those for the cyclization of the aminoacetone complex. The plot of k_{obs} vs. $[\text{OH}^-]$ is no longer linear but shows a curvature of decreasing slope. The limiting slope at low $[\text{OH}^-]$ leads to a rate constant for the production of carbinolamine of $1.3 \times 10^6 \text{ M}^{-1} \text{ s}^{-1}$. The fact that the plot is not linear is interpreted in terms of a change in the rate-determining step from condensation (at low $[\text{OH}^-]$) to the dehydration of the *gem*-diol (at high $[\text{OH}^-]$). These points are discussed in the following section.

Discussion

Synthesis (Scheme I). The reaction between $[\text{Co}(\text{NH}_3)_5(\text{Me}_2\text{SO})](\text{ClO}_4)_3$ and 1-amino-2-propanol in Me_2SO yielded $[\text{Co}(\text{NH}_3)_5\text{O}(\text{H})\text{CH}(\text{CH}_3)\text{CH}_2\text{NH}_2]^{2+}$ and $[\text{Co}(\text{NH}_3)_5\text{NH}_2\text{CH}_2\text{CH}(\text{OH})\text{CH}_3]^{3+}$ (I) in approximately equal quantities, and separation of these species was readily achieved through fractional crystallization of the perchlorate salts. An analogous synthesis (IX) using the more sterically hindered amino alcohol, 2-amino-1-phenylethanol, required a longer reaction time at a slightly elevated temperature to effect coordination of the ligand, and only the N-bound isomer was detected.

The conversion of coordinated amino alcohol to amino ketone (II, X) with acid-dichromate solutions occurred readily with little or no oxidation of the amine center. The coordinated aminoacetone complex (II) was also synthesized through the reaction of 2-(aminomethyl)-2-methyl-1,3-dioxalan^{2d} and $[\text{Co}(\text{NH}_3)_5\text{Me}_2\text{SO}](\text{ClO}_4)_3$ in Me_2SO , followed by acid-catalyzed removal of the ketal protecting group of the $[\text{Co}(\text{NH}_3)_5(\text{NH}_2\text{CH}_2\text{C}(\text{CH}_3)\text{OCH}_2\text{CH}_2\text{O})]^{3+}$ complex formed in situ. Treatment of these amino ketone complexes with base leads to an intramolecular capture of the carbonyl group by a deprotonated

Scheme I



cis ammine center to give the bidentate aminocarbinol chelate (IV). A subsequent base-catalyzed reaction produces the imine complexes (V, XI) quantitatively.

Similar chemistry was anticipated for more complicated molecules, and the strategy was employed to synthesize a multidentate ligand on the metal ion (Scheme II). In the example chosen, several isomeric possibilities existed and the experiment probes the factors which determine where and with what specificity the cyclization occurs.

The reaction between $(RR,SS)\text{-}\alpha\text{-}[\text{Co}(\text{trien})(\text{Cl})_2]\text{Cl}$ and aminoacetaldehyde dimethyl acetal in methanol yields $(RR,SS)\text{-}\alpha\text{-}[\text{Co}(\text{trien})(\text{NH}_2\text{CH}_2\text{CH}(\text{OCH}_3)_2)\text{Cl}]^{2+}$ (XII) as the only dipositive species. The same product was also obtained when $(RR,SS)\text{-}\beta\text{-}[\text{Co}(\text{trien})(\text{Cl})_2]\text{Cl}$ was substituted as the reactant.³⁹ The conversion of the coordinated dimethyl acetal to the aldehyde (XIII) in acidic solution is consistent with the usual acid-catalyzed path observed in organic chemistry.

Treatment of the $\alpha\text{-}[\text{Co}(\text{trien})(\text{NH}_2\text{CH}_2\text{CHO})\text{Cl}]^{2+}$ ion with base leads to the capture of the carbonyl group by the deprotonated secondary amine center trans to coordinated Cl⁻ to give the quinquidentate carbinolamine ligand arranged about the Co(III) ion in the configuration shown (XIV) (Figures 3 and 4). This

reaction can be conducted without loss of the Cl⁻ ion so that the parent configuration is preserved. Subsequent oxidation of the carbinolamine with Cr₂O₇²⁻ ion leads to the formation of the tertiary amide (XV), and the Cl⁻ ion remains coordinated. The crystallographic analysis clearly establishes the structure of the carbinolamine product. It also confirms the assignment of the configuration for the amino dimethyl acetal and aminoacetaldehyde complexes and establishes the configuration of the [Co(trenenone)Cl]²⁺ ion derived from the oxidation of the carbinolamine.

The coordinated tertiary amide (XV) is unusual since coordination of the N atom clearly restricts delocalization of charge over the

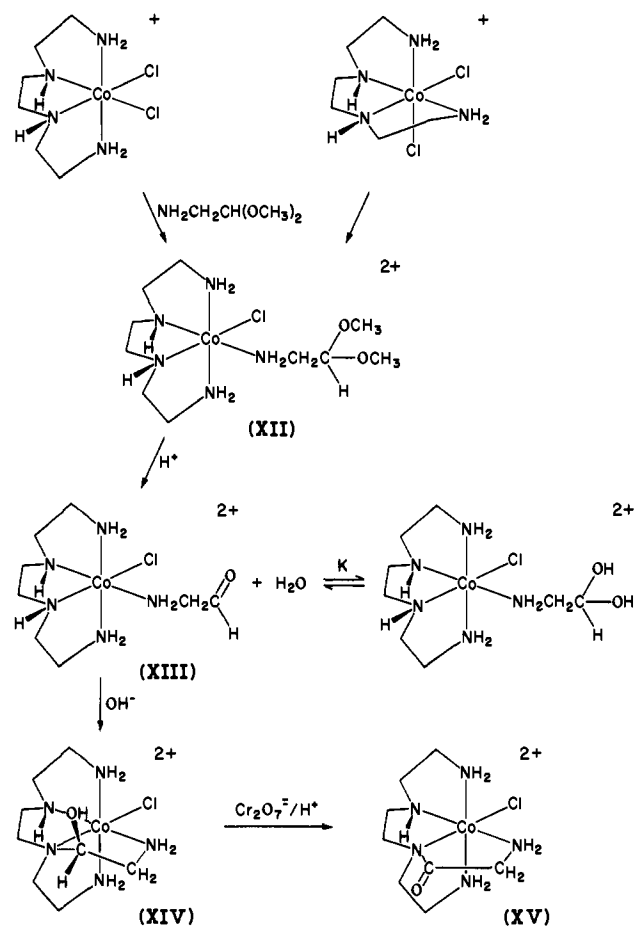


moiety. Usually, amides coordinate with the loss of a proton from the amide N atom to avoid this problem, and we are not aware of any instance where amide -NH₂ or -NHR centers are established as being coordinated through the N atom without deprotonation occurring. Such centers could behave more like ketone carbonyl groups and may react in like vein. For example, the stretching frequency for the >C=O group (1706 cm⁻¹) is closer to that of saturated ketones (~1700 cm⁻¹) than that of tertiary amides (~1650 cm⁻¹).

One important common feature of the various syntheses carried out is the role of the Co(III) center. The bound aminoacetone,

(39) Meisenheimer, J.; Kiderlen, E. *Justus Liebigs Ann. Chem.* **1924**, *438*, 241. Bailar, J. C.; Clapp, L. B. *J. Am. Chem. Soc.* **1945**, *67*, 171. The reaction with aminoacetaldehyde diethyl acetal under the same conditions yields $(RR,SS)\text{-}\beta_2\text{-}[\text{Co}(\text{trien})(\text{NH}_2\text{CH}_2\text{CH}(\text{OC}_2\text{H}_5)_2)\text{Cl}]\text{Cl}_2$ exclusively.

Scheme II



aminoacetophenone, and aminoacetaldehyde do not undergo polymerization because the amine center is protected by the metal ion. Co(III) is more effective than a proton in preventing intermolecular condensation since the ligands do not leave the metal ion during the reaction even in alkaline solution. Similarly, in the several ligand oxidations which were carried out (II, X, XV) the N protons are inert to exchange in the acidic conditions and the various ligand amine groups are also protected from the powerful oxidant, $\text{Cr}_2\text{O}_7^{2-}$, by coordination to the metal ion. This type of protection has some general synthetic utility.

The condensation of α -[Co(trien)($\text{NH}_2\text{CH}_2\text{CHO}$)Cl] $^{2+}$ to produce *t*-[Co(trenenol)Cl] $^{2+}$ is a reaction with interesting stereochemical possibilities. A significant result is that the intramolecular condensation reaction is regiospecific, condensation occurring only with the secondary amine center, not with the equally accessible *cis* primary amine centers. The regiospecificity is indicated in Scheme II and confirmed by the crystal structure determination (Figures 3 and 4). The ^1H NMR data for *cis*- and *trans*-[Co(en) $_2$ (NH_3)Cl] $^{2+}$ and *cis*-[Co(en) $_2$ ($\text{NH}_2\text{CH}_2\text{CH}(\text{OCH}_3)_2$)Cl] $^{2+}$ indicate that the N-H center *trans* to coordinated Cl $^-$ is by far the most acidic amine moiety.⁴⁰ The proton-exchange behavior for the N protons on the aldehyde complex should be similar, and the specificity for the site of the condensation is thereby accommodated.

Mechanism. The rate law for the cyclization of [Co(NH_3) $_5$ ($\text{NH}_2\text{CH}_2\text{COCH}_3$)] $^{3+}$ is simply first order in complex ion and first order in OH^- . Proton exchange also has the same rate law and was demonstrated to be twofold faster than the condensation under identical conditions. The derived rate law for the condensation process depicted in Figure 8, using the steady-state approximation, takes the form of

$$k_{\text{obsd}} = k_{\text{OD}}k_1[\text{OH}^-]/(k_{\text{D}_2\text{O}} + k_1) \quad (1)$$

$$k_c = k_{\text{OD}}k_1/(k_{\text{D}_2\text{O}} + k_1)$$

The deprotonation rate constant $k_{\text{OD}} = 3.0 \times 10^6 \text{ M}^{-1} \text{ s}^{-1}$ implies a rate constant for $k_{\text{D}_2\text{O}}$ of $\sim 10^8 \text{ s}^{-1}$ if the $\text{p}K_a$ of the amine center⁴¹

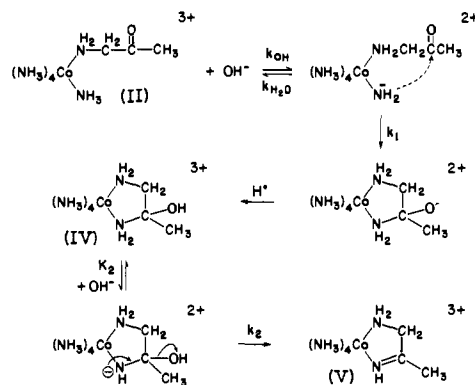


Figure 8. Proposed mechanism for the consecutive reactions of [Co(NH_3) $_5$ ($\text{NH}_2\text{CH}_2\text{COCH}_3$)] $^{3+}$ ion.

is ~ 16 . The observed cyclization rate constant k_c of $1.5 \times 10^6 \text{ M}^{-1} \text{ s}^{-1}$ under the same conditions then leads to an estimate of k_1 of $\sim 10^8 \text{ s}^{-1}$. The deprotonated chelated carbinolamine anion so formed (Figure 8) is likely to have a very basic oxygen atom ($\text{p}K_a \approx 14$) compared with uncoordinated carbinolamines and protonation by H_2O or other acids in aqueous solution is therefore likely to be very fast.⁴²

The absence of general-base catalysis can be accommodated readily. This property is not observed for proton exchange with the cobalt(III) pentaammine nor with hexaammine complexes. Neither should it be observed for the intramolecular cyclization of the coordinated amido ion at the carbonyl group. The amido ion is a very basic group ($\text{p}K_a \approx 16$) and there is no requirement for proton transfer from the amine group to the oxygen anion in the product carbinolamine anion. Protonation of the basic oxygen would come from H_2O or buffer acid, and since no acid catalysis was observed, we presume the protonation is fast relative to the other steps.

Subsequent to the condensation step (k_1) elimination of water to give the imine was observed. Deprotonation of the [Co(NH_3) $_4$ ($\text{NH}_2\text{CH}_2\text{C}(\text{OH})\text{CH}_3\text{NH}_2$)] $^{3+}$ ion (IV) at the amine center adjacent to the chiral carbon atom ($\text{p}K_a \approx 16$) to give a coordinated amido ion allows OH^- to leave the residual neutral imine moiety. Here the proton-exchange rate is much faster than OH^- loss, and the rate law takes the form

$$k_{\text{obsd}} = k_2K_2[\text{OH}^-] = k_1[\text{OH}^-] \quad (2)$$

Equating the observed and derived rate laws yields $k_2K_2 = k_1 = 1.12 (\pm 0.15) \times 10^4 \text{ M}^{-1} \text{ s}^{-1}$ at 25°C , $\mu = 1.0$. Assuming K_2 for deprotonation by OH^- as $\sim 10^{-2} \text{ M}^{-1}$ as before allows an estimate of $k_2 \approx 10^6 \text{ s}^{-1}$ for the elimination reaction. The implication in this analysis is that the elimination is not concerted with proton removal.

These results need to be compared with the same type of reactions in the absence of the metal complexes. Similar reactions in organic chemistry are often subject to general acid-base catalysis and it is unusual that the formation of both carbinolamine and imine can be observed as discrete rate steps. Carbinolamine formation is often very fast⁴³ in organic chemistry because it is possible for the amine to attack the carbonyl center directly. For the Co(III) complexes, reaction requires that the coordinated amine be deprotonated prior to condensation with the carbonyl center. The slower rates observed are due to the low concentration of the deprotonated nucleophile in neutral and acidic solutions. The absence of general acid-base catalysis in the formation of the coordinated carbinolamine has been discussed above.

The (slower) dehydration of the coordinated carbinolamine to form a coordinated imine also requires the deprotonation of the coordinated carbinolamine amine group by hydroxide ion. In

(40) Buckingham, D. A.; Marzilli, P. A.; Sargeson, A. M. *Inorg. Chem.* **1969**, *8*, 1595. Gainsford, A. R.; Sargeson, A. M., unpublished results.

(41) (a) Buckingham, D. A.; Marzilli, L. G.; Sargeson, A. M. *J. Am. Chem. Soc.* **1967**, *89*, 825 and references therein. (b) Sargeson, A. M. *Pure Appl. Chem.* **1973**, *33*, 527.

(42) Eigen, M. *Angew. Chem., Int. Ed. Engl.* **1964**, *3*, 1.

(43) Diebler, H.; Thorneley, R. N. P. *J. Am. Chem. Soc.* **1973**, *95*, 896.

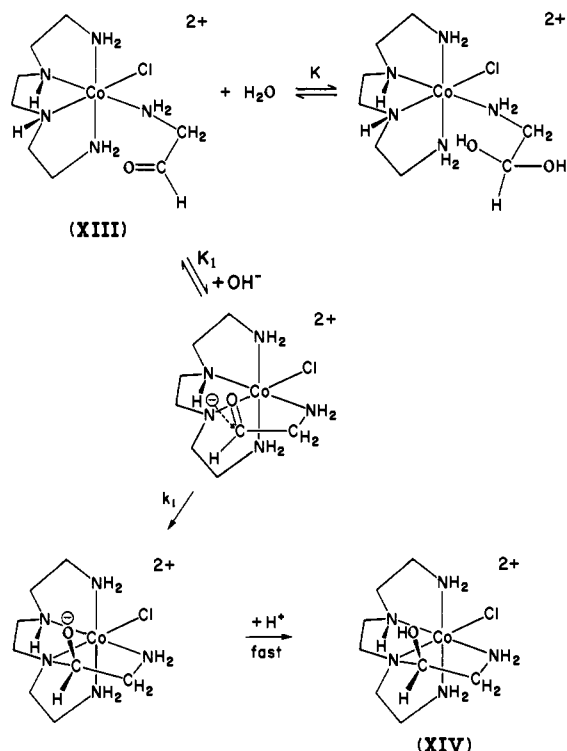


Figure 9. Proposed reaction mechanism for the base-catalyzed condensation of $(RR,SS)\text{-}\alpha\text{-[Co(trien)(NH}_2\text{CH}_2\text{CHO)Cl]}^{2+}$ ion.

organic chemistry the subsequent elimination of hydroxide to produce the imine is frequently general acid catalyzed.⁴⁴ A possible explanation for the absence of acid catalysis here is that the carbinolamine OH is not sufficiently basic to be protonated by the acids available (H_2O , pyridinium ion, or imidazolium ion). Also the cationic acids employed in the study are less able to approach the cationic complex in order to effect proton transfer to the leaving OH^- group. Certainly there is no acid-catalyzed path in the range of the measurements even though the buffer acids used are $10^7\text{--}10^8$ -fold more acidic than H_2O .

One striking feature of the chemistry is the ease with which the carbinolamine complex can be isolated and stabilized. There is a possibility that this ion could be resolved into its catoptric forms and the rate of loss of chirality relative to imine formation determined. Such an experiment would be another means of probing the elimination.

The intramolecular condensation of $(R,S)\text{-}\alpha\text{-[Co(trien)(NH}_2\text{CH}_2\text{CHO)]}^{2+}$ to produce a carbinolamine displays more complicated kinetics than the aminoacetone complex. A plot of k_{obsd} against $[\text{OH}^-]$ for this reaction (Figure 7) is not linear, and there is a marked effect of buffer type and concentration on the observed rate constant.⁴⁵ One significant difference between the aminoacetaldehyde and aminoacetone reactions is that ^1H NMR data (Figure 2) show that the coordinated aminoacetaldehyde is predominantly hydrated as the *gem*-diol form. The equilibrium constant $K = \text{diol/aldehyde} = 10 \pm 2$. In D_2O the equilibrium is established rapidly⁴⁵ in near neutral and acid conditions. However, infrared spectra of the solid isolated complex indicate at least some free aldehyde ($\nu_{\text{C=O}} = 1715\text{ cm}^{-1}$). The fact that the plot of k_{obsd} against $[\text{OH}^-]$ for the pH-stat experiments (Figure 7) is not linear suggests that there may be a change in the rate-determining step over the pH range studied. A plausible explanation consistent with the complex chemistry and organic diol chemistry is that carbinolamine formation is rate determining at low pH and elimination of H_2O from the diol is rate determining at high pH.

A mechanism consistent with this proposal is shown in Figure 9. At low $[\text{OH}^-]$ nucleophilic attack of the deprotonated amine (trans to Cl^-) at the carbonyl center of the free aldehyde can be argued as the rate-determining step for the condensation (k_1) since N-H exchange is much faster than carbinolamine formation. The rate law derived for this path takes the form

$$k_{\text{obsd}} = k_1 K_1 [\text{OH}^-] / (1 + K) \quad (3)$$

This differs from the rate law for the condensation reaction of aminoacetone (1) in that it contains a denominator which is related to the aldehyde/*gem*-diol equilibrium (K). It predicts a linear dependence of k_{obsd} on $[\text{OH}^-]$. The limiting slope at low $[\text{OH}^-]$ is $1.2 \times 10^5\text{ M}^{-1}\text{ s}^{-1}$. From the rate law (3) this is equal to $k_1 K_1 / (1 + K)$. Estimates for K_1 , deprotonation of the amine with OH^- , and K , *gem*-diol/aldehyde equilibrium constant, are probably $\sim 10^{-2}$ and ~ 10 , respectively. This leads to an estimate of $k_1 \approx 10^8\text{ s}^{-1}$.

As $[\text{OH}^-]$ increases, there is a shift in rate-determining step to dehydration of the *gem*-diol. This is consistent with the general hydration-dehydration chemistry of aldehydes.⁴⁶ The rate constant for dehydration of the *gem*-diol is $k_{\text{obsd}} = k_0 + k_{\text{OH}^-}[\text{OH}^-]$; k_0 represents the rate constant for the uncatalyzed path and k_{OH^-} that for the specific OH^- ion-catalyzed path. At high $[\text{OH}^-]$ this is the rate-determining step, and a plot of k_{obsd} against $[\text{OH}^-]$ should be linear with an intercept equal to k_0 and a slope equal to k_{OH^-} . From the pH-stat experiments a limiting slope can only be estimated. The reaction was too fast to study at higher pH by this technique, and the measured slope represents a maximum slope since the curve could possibly level off at high pH. The plot therefore yields an upper limit for k_{OH^-} and a lower limit for k_0 . From Figure 7, $k_{\text{OH}^-} \leq 1.9 \times 10^4\text{ M}^{-1}\text{ s}^{-1}$ and $k_0 \geq 4.5 \times 10^{-3}\text{ s}^{-1}$. These values are in accord^{46b} with analogous rate constants for dehydration of uncoordinated *gem*-diols.

Additional evidence for the notion that the curvature in Figure 7 is related to a shift in rate-determining step comes from the dependence of the reaction rate on buffer $\text{p}K_a$ and buffer concentration. This behavior is consistent with the general-acid-base dependence observed in the *gem*-diol/aldehyde hydration-dehydration reactions. However, it is not consistent with the chemistry associated with attack of coordinated amido ions at carbonyl centers as observed for the aminoacetone cyclization. Since the buffer effects are unrelated to the general chemistry in this article, they are not pursued further but the kinetic data are available if required.⁴⁵

Efficiency of the Condensation Reaction. The rate constants for the condensation reactions can be compared with the rate constants for proton exchange at the relevant amine centers and the efficiency of capture of the carbonyl group determined. Cyclization of the aminoacetone complex occurs with a rate constant of $1.47 \times 10^6\text{ M}^{-1}\text{ s}^{-1}$ and proton exchange of the *cis* amines at $3.0 \times 10^6\text{ M}^{-1}\text{ s}^{-1}$. Therefore, the ketone is captured by every other proton exchange which is extraordinarily efficient considering the ratio of H_2O molecules to the carbonyl group ($\sim 50:1$).

The condensation process for $(R,S)\text{-}\alpha\text{-[Co(trien)(NH}_2\text{CH}_2\text{CH(OH)}_2\text{)Cl]}^{2+}$ is less efficient. The condensation rate constant ($k_1 K_1 = 1.3 \times 10^6\text{ M}^{-1}\text{ s}^{-1}$) is significantly less than that for proton exchange at the secondary amine center trans to bound Cl^- ($4 \times 10^7\text{ M}^{-1}\text{ s}^{-1}$ at 25°C) assuming that the latter is the same for the *gem*-diol and the aldehyde forms of the complex. The aldehyde is captured about once in 30 proton exchanges. Similar efficiencies have been observed in base-catalyzed condensations of *cis*- $[\text{Co(en)}_2(\text{NH}_2\text{CH}_2\text{CN)Cl}]^{2+}$ to give a chelated amidine⁴⁷ and *cis*- $[\text{Co(en)}_2(\text{NH}_2\text{CH}_2\text{C(=O)CH}_3)]^{2+}$ to give a chelated carbinolamine.^{2d} Presumably the efficiency arises from the intramolecularity of the process and the rate gain arises largely from loss of translational entropy.⁴⁸ For the pentaamine conden-

(44) Sayer, J. M.; Jencks, W. P. *J. Am. Chem. Soc.* **1977**, *99*, 464 and earlier references therein.

(45) These data are deposited separately. See Supplementary Material Available.

(46) (a) Ahrens, M. L.; Maass, G.; Schuster, P.; Winkler, H. *J. Am. Chem. Soc.* **1970**, *92*, 6134. (b) Bell, R. P. *Adv. Org. Chem.* **1966**, *4*, 1.

(47) Buckingham, D. A.; Foxman, B. M.; Sargeson, A. M.; Zanella, A. *J. Am. Chem. Soc.* **1972**, *94*, 1007.

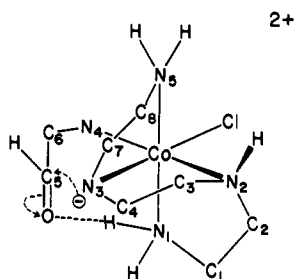


Figure 10. Proposed stereochemistry of the transition state in the base-catalyzed condensation of $(RR,SS)\text{-}\alpha\text{-[Co(trien)(NH}_2\text{CH}_2\text{CHO)Cl]}^{2+}$ ion.

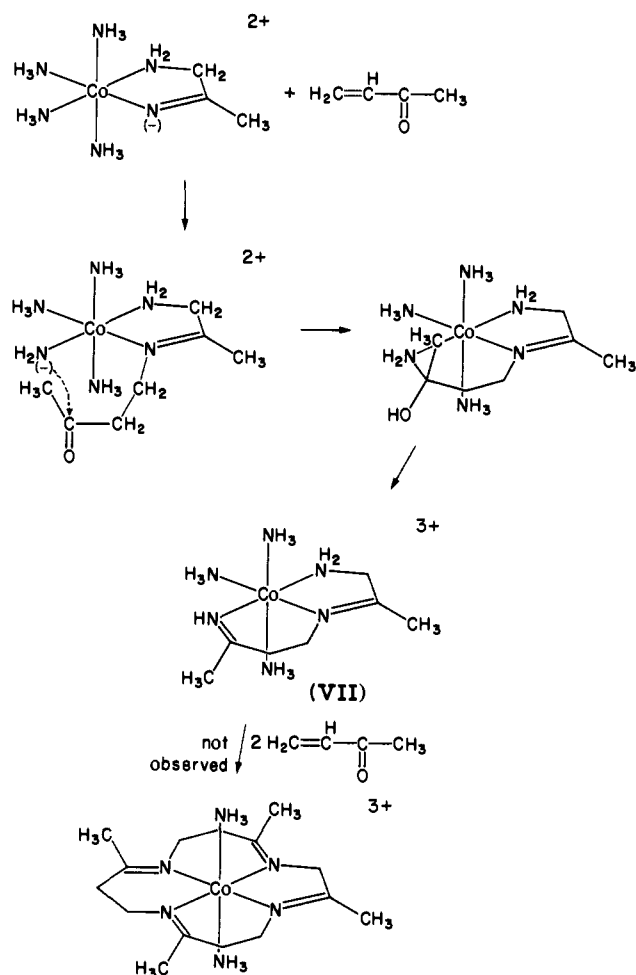
sations the nucleophile is essentially ubiquitous in its proximity to the $>\text{C}=\text{O}$ group and there is little rate loss from rotational or vibrational degrees of freedom. The triethylenetetramine complex is more restricted in that the concentration of the free carbonyl group is less. After the data are corrected for the hydration equilibrium, the efficiency of the capture is much the same as that for aminoacetone.

Stereochemistry. A most striking feature of the intramolecular condensation of the $(R,S)\text{-}\alpha\text{-[Co(trien)(NH}_2\text{CH}_2\text{CHO)Cl]}^{2+}$ ion is its high regio- and stereoselectivity. The aldehyde condenses only at the amine site trans to bound Cl^- and the carbinolamine appears to be stereospecific. The structural and NMR studies do not show any sign of other isomers. The reason for the regioselectivity has already been given, namely, that the N protons trans to bound Cl^- are much more acidic than those cis. The directing influence for the stereospecificity is less certain, but the existence of a short hydrogen bond from a proton on N(1) to the oxygen atom of the carbinolamine indicates that such a bond to the carbonyl oxygen might also exist in the activated complex. A feasible configuration for the activated complex is depicted in Figure 10. The carbonyl oxygen is directed at the proton of N(1). This orientation puts the coordinated amide ion in a favorable position to attack the carbonyl moiety. The H bond is retained in the product carbinolamine and probably holds the OH group in an axial position for the hydroxydiamine chelate.

It is interesting to consider these condensations in relation to a deprotonated chiral N center which can also racemize. Usually such centers invert $\sim 10^4\text{--}10^6$ -fold more slowly than the proton exchanges.³⁸ It follows that condensations of the type discussed here would be expected to occur largely with retention of configuration at the nucleophilic coordinated amide ion. This may in turn direct the stereochemistry of a chiral carbinolamine center. However, such questions have yet to be examined.

Reactions of the Imine $[\text{Co}(\text{NH}_3)_4\text{NH}=\text{C}(\text{CH}_3)\text{CH}_2\text{NH}_2]^{3+}$ Ion. ¹H NMR data indicate that exchange of the methylene protons is at least 200-fold faster than exchange of the methyl protons. The imine N proton is much more acidic than the ammine protons or the methylene and methyl protons. It is therefore easy to generate the imine N anion and methyl vinyl ketone adds to it readily through the terminal olefin C atom. In the basic conditions for the reaction, a deprotonated adjacent ammine group then attacks the carbonyl function to give first the carbinolamine and then the imine. The tridentate so produced has the potential to add successively two methyl vinyl ketone residues at the terminal imine centers to produce (Scheme III) a 5,6,6,6 ring macrocycle (a corrin precursor). However, at least in aqueous solution decomposition of the reactants occurred before the macrocycle was formed. The decomposition arises probably from deprotonation at the imine N and/or the methylene carbon centers which leads to reduction of the Co(III) ion by the N anion and/or the carbanion. At pH 12 the rate of decomposition is quite fast ($t_{1/2} \approx 10$ s).

Scheme III



The instability of the imine complex was somewhat disappointing from a synthetic point of view, but it does not preclude reduction of the imine by BH_4^- ion to the saturated amine complex $[(\text{NH}_3)_4\text{CoNH}_2\text{CH}_2\text{CH}(\text{CH}_3)\text{NH}_2]^{3+}$ (VI), albeit in low yield. Similarly, the carbanion generated by deprotonation of the methylene group condenses readily with formaldehyde to give the dimethylene hydroxy derivative (VIII). It is conceivable that the stabilities of the carbanion and nitrogen anion entities might increase in nonaqueous aprotic solvents but these factors have not yet been explored.

Acknowledgment. We are grateful for generous allocations of time on the Univac-1108 computer at the Computer Centre and for microanalysis by the Microanalytical Unit of the Australian National University. This material is partially based upon work supported by the National Science Foundation under Grant No. INT-7912374 (R.P.). R.P. also gratefully acknowledges partial support from the PSC/BHE Faculty Research Award Program of the City University of New York. The authors are also grateful for some pertinent comments from Professor W. P. Jencks which substantially improved the paper.

Supplementary Material Available: A listing of structure factor amplitudes and kinetic data for the conversion of $(RR,SS)\text{-}\alpha\text{-[Co(trien)(NH}_2\text{CH}_2\text{CHO)Cl]}^{2+}$ to $t\text{-[Co(trenenol)Cl]}^{2+}$ at 25 °C in various buffers and details of the base catalyzed cyclization of $[\text{Co}(\text{NH}_3)_5\text{NH}_2\text{CH}_2\text{COCH}_3]^{3+}$ and dehydration of $[\text{Co}(\text{NH}_3)_4\text{NH}_2\text{CH}_2\text{C}(\text{OH})(\text{CH}_3)\text{NH}_2]^{3+}$ (12 pages). Ordering information is given on any current masthead page.